# Illuminating N-acylethanolamine biosynthesis with new chemical tools

Mock, E.D.

# Chapter 4

## Photoaffinity probes for NAPE-PLD confirm LEI-401 target engagement

### 4.1 Introduction

Proof of target engagement is an important checkpoint in drug discovery.[1] Confirmation of the physical interaction between the drug candidate and the protein of interest in a biological setting, preferably in cells or in live animals, in combination with the desired phenotypic effect, validates the proposed mode of action of the drug and its intended target.[2] This speeds up the clinical translation of drug development, as full target engagement with the absence of a therapeutic effect will dismiss a drug for the intended disease indication. In practice, establishing such a binding event *in vivo* is oftentimes a difficult task. The costly failure of clinical candidates in Phase II and Phase III clinical trials has been attributed to a lack of efficacy, which in certain cases was accompanied by the inability to show engagement of the intended targets.[3]

The emergence of the field of chemical biology in combination with the technical advancement of tandem mass spectrometry, has drastically improved and facilitated target engagement studies.[4] In particular, activity based protein profiling (ABPP) and

photoaffinity labeling (PAL) are complementary techniques well suited to obtain ligand-protein binding information in cellular systems and living organisms.[5] ABPP takes advantage of the catalytic nucleophile of an enzyme to form an irreversible bond with an electrophilic chemical probe containing a ligation handle, which enables affinity purification and protein identification. Using competition experiments this has allowed validation of target engagement of drug candidates in several classes of enzymes including, amongst others, proteases, serine hydrolases and glycosidases.[5-9] In addition, the off-target landscape of a drug candidate within an enzyme family can be profiled using ABPP, providing important selectivity information.[10,11] A critical requirement of ABPP is that targeted enzymes form a covalent bond with their substrates and the active-site catalytic nucleophile, which is not the case for enzyme classes such as metallohydrolases.[12] Consequently, photoaffinity labeling has come to the foreground, as it can be applied to the complete proteome, even including proteins that do not possess any enzymatic activity.[13] This advantage has led to many new applications for PAL such as target identification of natural products[14,15] and small molecules[16], their protein binding site[17], lipid-protein[18,19] as well as protein-protein interactions[20].

Photoaffinity labeling utilizes a photoreactive group instead of an electrophile, that can be converted into a highly reactive intermediate with UV irradiation, thereby irreversibly inserting itself into side chain or backbone residues of the bound protein.[12] Analogous to ABPP, PAL probes contain an affinity group for optimal binding to the intended target and a ligation handle for click chemistry. The diazirine group has become a preferred photocrosslinker in recent years owing to its small size and its highly reactive, short-lived (~1 ns) singlet carbene intermediate which can insert into O-H, N-H and C-H bonds (Figure 1).[21-23] Furthermore, diazirines require low energy UV light (> 350 nm) for their photoactivation, minimizing damage to biological samples. Of note, labeling efficiencies of

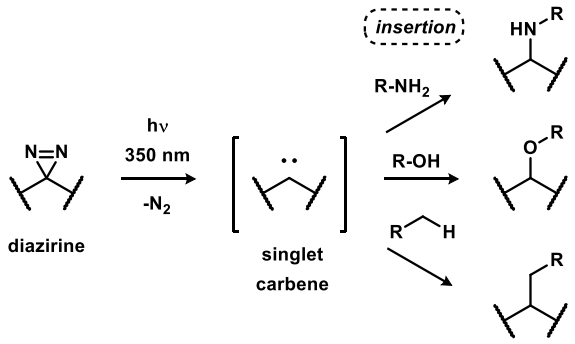


**Figure 1.** Photoactivation of diazirines with low-energy UV light generates a short-lived singlet carbene species that can insert into side chain or backbone residues of proteins.

small aliphatic diazirines with β-hydrogens are reduced compared to the bulkier trifluoromethylaryldiazirine, due to a competing 1,2-hydride shift side reaction which converts the carbene into an alkene.[24] The biological systems used for PAL at first predominantly consisted of purified proteins and lysates. Thanks to advances in bioorthogonal chemistry techniques (e.g. click chemistry), experiments have seen a shift towards intact cell settings.[25] Importantly, whole cells better imitate relevant physiological conditions, as factors such as protein localization, drug cellular permeability and biodistribution are taken into account, essential for establishing target engagement. A typical live cell PAL experiment is depicted in Figure 2. Cells are treated with a photoaffinity probe that will bind to its protein partners. A competitor, for example, a drug candidate on which the PAL probe is based, can be pre-incubated to reversibly compete out the probe from the binding site. Upon photoirradiation the photoprobe will covalently bind to the protein binding site, thereby making a snapshot of the cellular probe-target binding equilibrium. Lysis of the cells, followed by attachment of a fluorophore or biotin handle via click chemistry, allows identification of the targeted proteins and can demonstrate target engagement by the competing drug candidate. PAL probes have successfully been used to target a growing list of proteins, which include metalloproteases[26], kinases[27], γ-secretase[28], methyltransferases[29], GPCRs[30], and histone deacylases[31]. Currently, the required UV irradiation for activation of the photoreactive groups, limits the use of PAL in whole organisms as a result of the restricted tissue penetration of UV light. Recent studies in translucent zebrafish[32] as well as intracranial photoactivation in mice using a fiber-optic cable[33], further increase the scope of PAL for *in vivo* use.

In this chapter, the development of photoaffinity probes for the enzyme *N*-acylphosphatidylethanolamine phospholipase D (NAPE-PLD) is described. NAPE-PLD

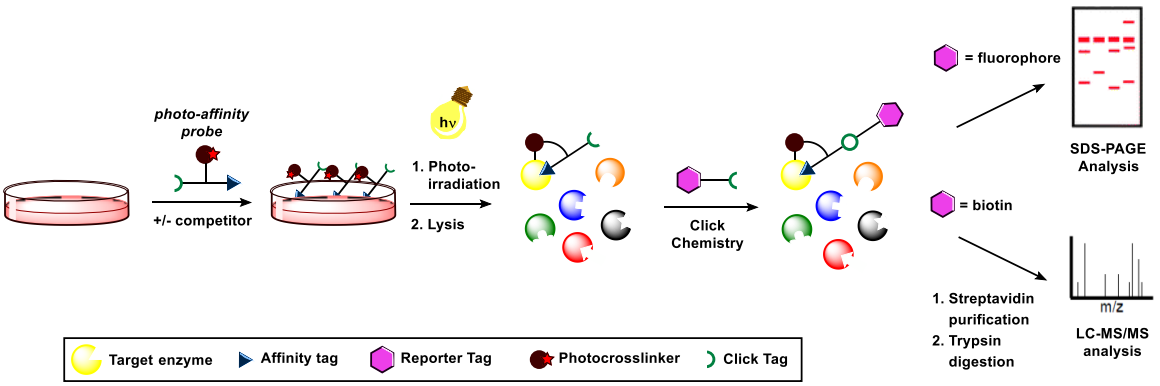


**Figure 2.** General work-flow of a live cell photoaffinity labeling experiment.

catalyzes the production of a family of signaling lipids called *N*-acylethanolamines (NAEs) from their NAPE precursors.[34] NAPE-PLD has a metallo-β-lactamase fold and contains two zinc ions in its active site that coordinate a water molecule which hydrolyzes the phosphodiester bond of NAPE.[35] To confirm cellular target engagement of *in vitro* active NAPE-PLD inhibitors, a photoaffinity labeling assay was realized. For the design of the PAL probes two strategies were investigated: stabilized analogues of the natural substrate NAPE and photoactivatable probes based on the pyrimidine-6-carboxamide NAPE-PLD inhibitor series described in Chapter 3. Unfortunately, the NAPE-based probes were ineffective in labeling NAPE-PLD, whereas the pyrimidine-based probes **50** and **51** were able to visualize NAPE-PLD *in situ* in transfected HEK293T cells overexpressing this enzyme. Using these pyrimidine-based probes, cellular binding of **LEI-401** with NAPE-PLD was confirmed, thereby providing evidence for its target engagement.

## 4.2 Results

### 4.2.1 Design and synthesis of NAPE-based photoprobes.

The design of the photoprobes was inspired by a previous report of a racemic phosphoramidate NAPE mimic, which had reasonable inhibitory activity for NAPE-PLD ($IC_{50}$ = ~10 μM).[36] Incorporation of this phosphoramidate group in combination with a photoreactive aliphatic diazirine group and an alkyne fatty acid, gave photoprobe **1** (Figure 3). A short *N*-pentyl photocrosslinking acyl chain was chosen due to synthetic accessibility from levulinic acid, while retaining affinity for NAPE-PLD.[37] Different phosphodiester bioisosteres containing one or two sulfur atoms, that can potentially coordinate to the active site zinc ions, were incorporated into the design for probes **2-5**, to investigate their influence on the NAPE-PLD inhibitory activity. The photocrosslinker and click tag were placed on the *N*-acyl fatty acid to circumvent phospholipase-mediated loss of labeling signal by hydrolysis of the ester group. In addition, the fatty acids of the phosphatidylethanolamine were selected based on their predominant natural occurrence.[38] Lastly, the influence of the diazirine position on the labeling efficiency of NAPE-PLD was investigated with probes **4, 6** and **7.**

The synthesis of probe **1** is shown in Scheme 1. Generation of 15-hexadecynoic acid (**12**) was achieved in four steps starting from 15-hydroxypentadecanoic acid (**8**). First, the carboxylic was esterified followed by oxidation of the alcohol to the aldehyde with pyridinium chlorochromate (PCC). Next, the alkyne was installed using the Ohira-Bestmann reagent[39] and the ester was hydrolyzed, affording fatty acid **12**. Utilizing a

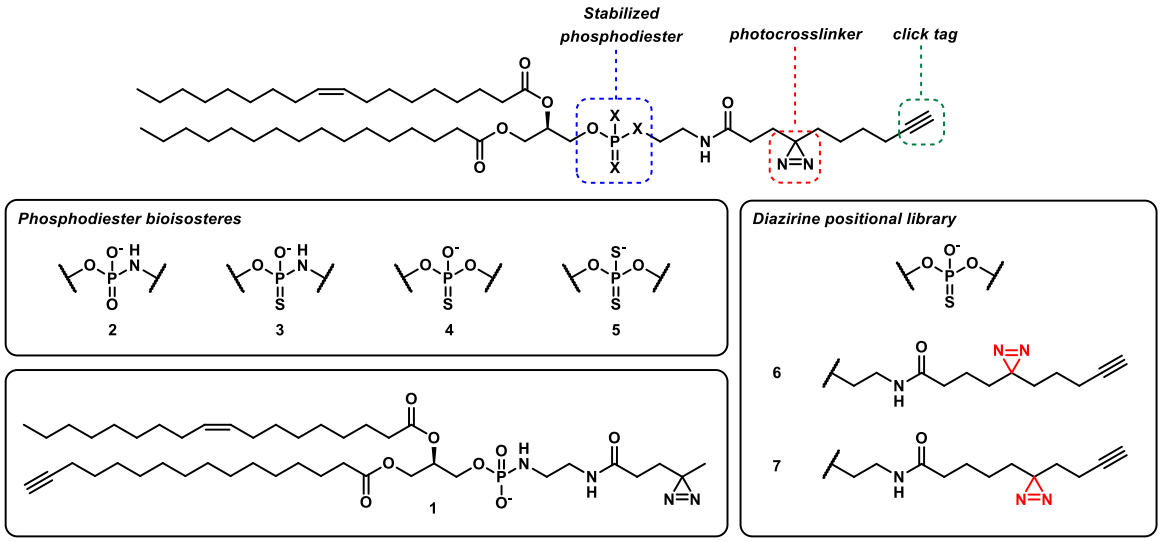


**Figure 3.** Design of NAPE-based photoaffinity probes **1-7**, incorporating a stabilized phosphodiester, a photoreactive diazirine and an alkyne ligation handle.

two-step one-pot sequence described by Minnaard and co-workers[40], **12** was treated with TBDMS-protected (*R*)-glycidol to give regioselective opening of the epoxide with (*S*,*S*)-Co(salen) as a catalyst. Esterification of the secondary alcohol with oleic acid delivered the mixed 1,2-diacylglycerol **13**. Mild deprotection of the TBDMS group to afford **14** was achieved with $Et_3N{\cdot}3HF$ in highyield, with no rearrangement to the 1,3-diacylglycerol observed. Phosphoramidite **15** was generated using standard phosphor coupling conditions. Next, amine **19** was synthesized in three steps, starting from levulinic acid (**16**), which was converted to the diazirine **17** using a three-step one pot procedure.[41] This involved treatment with ammonia in methanol followed by hydroxylamine-*O*-sulfonic acid to form the diaziridine and subsequent oxidation with iodine and triethylamine to form diazirine **17**. Subsequent amide coupling with Boc-ethylenediamine and Boc deprotection afforded **19**. To form the desired phosphoramidate bond an Atherton-Todd coupling was envisioned. Phosphoramidite **15** was converted to the *H*-phosphonate after which treatment with tetrachloromethane, triethylamine and amine **19** gave phosphoramidate **20**. Deprotection of the cyanoethyl group afforded the final product **1**.

To circumvent NAPE-PLD- or phospholipase-mediated hydrolysis of the photoprobe, resulting in release of the alkyne from the photocrosslinker, bifunctional fatty acids were incorporated as the *N*-acyl group. Three different ω-alkyne diazirine fatty acids (**33**-**35**) were prepared to probe the optimal site of the photocrosslinker (Scheme 2). A modular synthesis was developed using commercially available ω-alkyne fatty acids **21**-**23**, which were converted to β-ketoesters **24**-**26** via coupling with Meldrum's acid followed by reflux

in methanol or ethanol. Alkylation with methyl bromoacetate for **24** or ethyl 4-bromobutanoate for **26** afforded diesters **27** or **29**, respectively. Diester **28** was generated via Michael addition of methyl acrylate and β-ketoester **25**. Subsequent hydrolysis and decarboxylation afforded the γ-ketoacids **30**-**32**. Using a similar three-step one-pot procedure as for levulinic acid, ketoacids **30**-**32** were transformed to diazirines **33**-**35**. **33** was coupled with Boc-ethylenediamine and deprotected to form amine **37**. Alternatively, carboxylic acids **30**-**32** were condensed with ethanolamine to generate ethanolamides **38**-**40**.

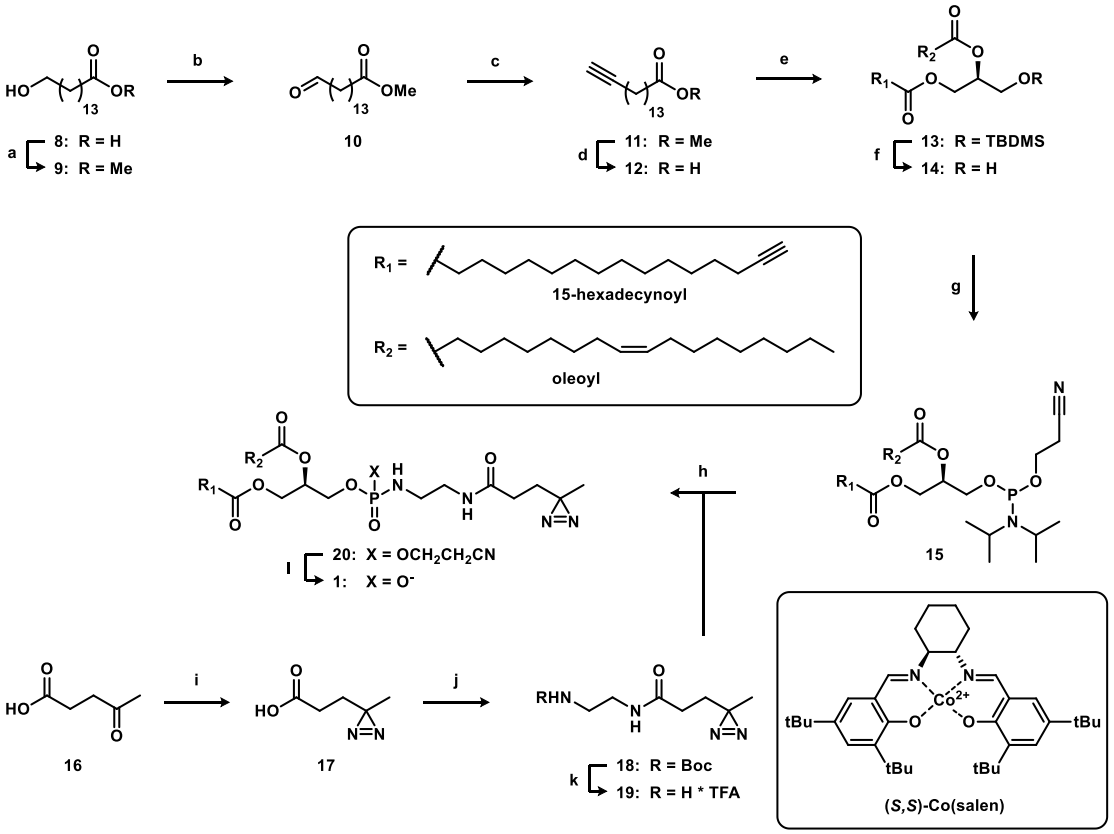


**Scheme 1.** Synthesis of photoprobe **1**. Reagents **a**nd conditions: a) AcCl, MeOH, 83%; b) PCC, DCM, 74%; c) dimethyl (1-diazo-2-oxopropyl)phosphonate (Ohira-Bestmann reagent), $K_2CO_3$, MeOH, 0 °C to rt, 40%; d) NaOH, THF, $H_2O$, 99%; e) *i*. (*R*)-*tert*-butyldimethyl(oxiran-2-ylmethoxy)silane, (*S*,*S*)-Co(salen), DiPEA, $O_2$; *ii*. oleic acid, DIC, DMAP, heptane, 0 °C to rt, 35%; f) $Et_3N{\cdot}3HF$, THF, $CH_3CN$, 93%; g) 2-cyanoethyl *N*,*N*-diisopropylchlorophosphoramidite, DiPEA, DCM, 98%; h) *i*. 1*H*-tetrazole, $CH_3CN$, $H_2O$; *ii*. **19**, $CCl_4$, $Et_3N$, $CH_3CN$, 55%; i) *i*. 7 M $NH_3$ in MeOH, 0 °C; *ii*. $NH_2O(SO_3H)$, 0 °C to rt; *iii*. $I_2$, $Et_3N$, MeOH, 0 °C to rt, 47%; j) *i*. *N*-hydroxysuccinimide, EDC·HCl, $Et_3N$, DCM, ii. *N*-Boc-ethylenediamine, 71%; k) TFA, DCM, 99%, l) DBU, DCM, 41%.

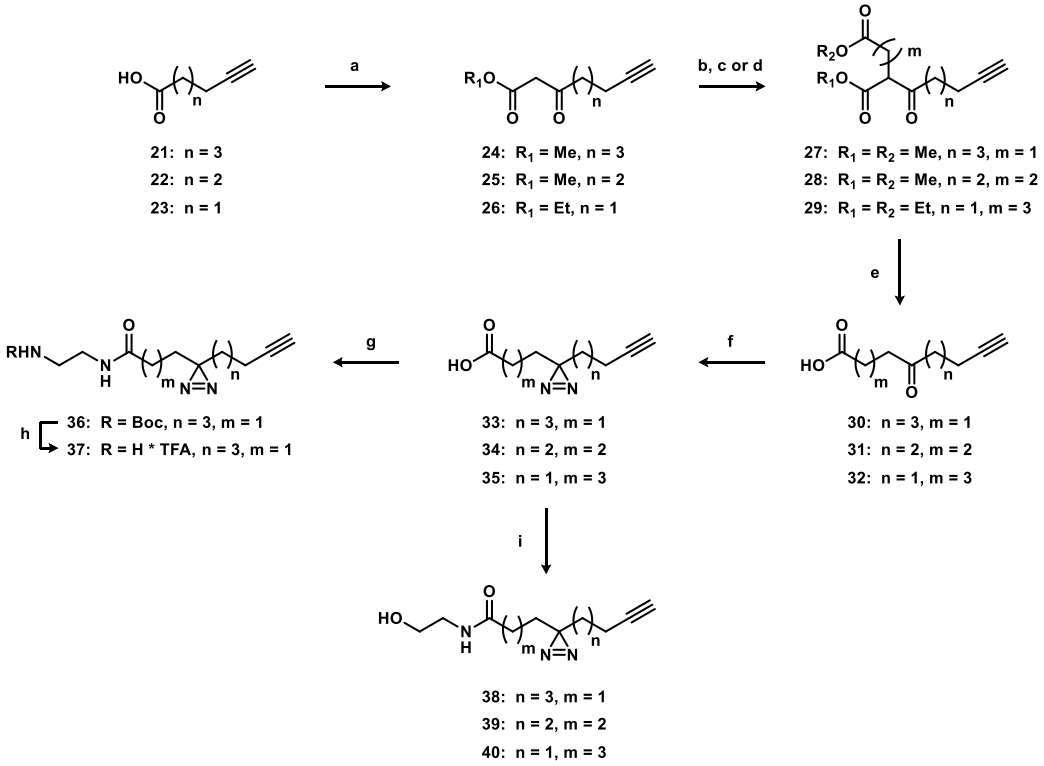


**Scheme 2.** Synthesis of bifunctional fatty acids **33-35**. Reagents and conditions: a) *i.* Meldrum's acid, DIC, DMAP, DCM; *ii*. MeOH or EtOH, reflux, **24**: 74%, **25**: 52%, **26**: 58%; b) for **27**: **24**, methyl bromoacetate, NaOMe, MeOH, 66%; c) for **28**: **25**, methyl acrylate, $K_2CO_3$, DCM/DMF, 53% d) for **29**: **26**, ethyl 4-bromobutanoate, NaOEt, EtOH, 38%; e) *i*. NaOH, THF, $H_2O$; *ii*. HCl, 0 °C to 55 °C, **30**: 99%, **31**: 84%; **32**: 82%; f) *i*. 7 M $NH_3$ in MeOH, 0 °C; *ii*. $NH_2O(SO_3H)$, 0 °C to rt; *iii*. $I_2$, $Et_3N$, MeOH, 0 °C to rt, **33**: 51%, **34**: 55%; **35**: 38%; g) *N*-Boc-ethylenediamine, EDC·HCl, HOBt, DCM, 97%; h) TFA, DCM, 99%; i) ethanolamine, EDC·HCl, HOBt, DCM, **38**: 78%, **39**: 76%, **40**: 69%.

Next, *sn*-1-palmitoyl-*sn*-2-oleoylglycerol **43** was prepared in three steps using an analogous route as for **14** (Scheme 3). Installation of the phosphoramidite with standard $P^{III}$ chemistry afforded key intermediate **44**. Using a similar Atherton-Todd procedure as for probe **1**, phosphoramidite **44** was converted to the *H*-phosphonate and coupled with amine **37** to generate phosphoramidate **45**. Deprotection with DBU gave photoprobe **2**. As the phosphoramidate moiety is known to be labile under acidic conditions, synthesis of a more stable thiophosphoramidate was explored.[42] A solution of hydrogen sulfide in THF was used to generate the *H*-thiophosphonate from **44**, that was converted to the desired thiophosphoramidate **46** with amine **37** using Atherton-Todd conditions. Deprotection of the cyanoethyl group with *tert*-butylamine to scavenge the liberated acrylonitrile, that could potentially react with the nucleophilic sulfur, afforded thiophosphoramidate **3** as a mixture of two diastereomers.

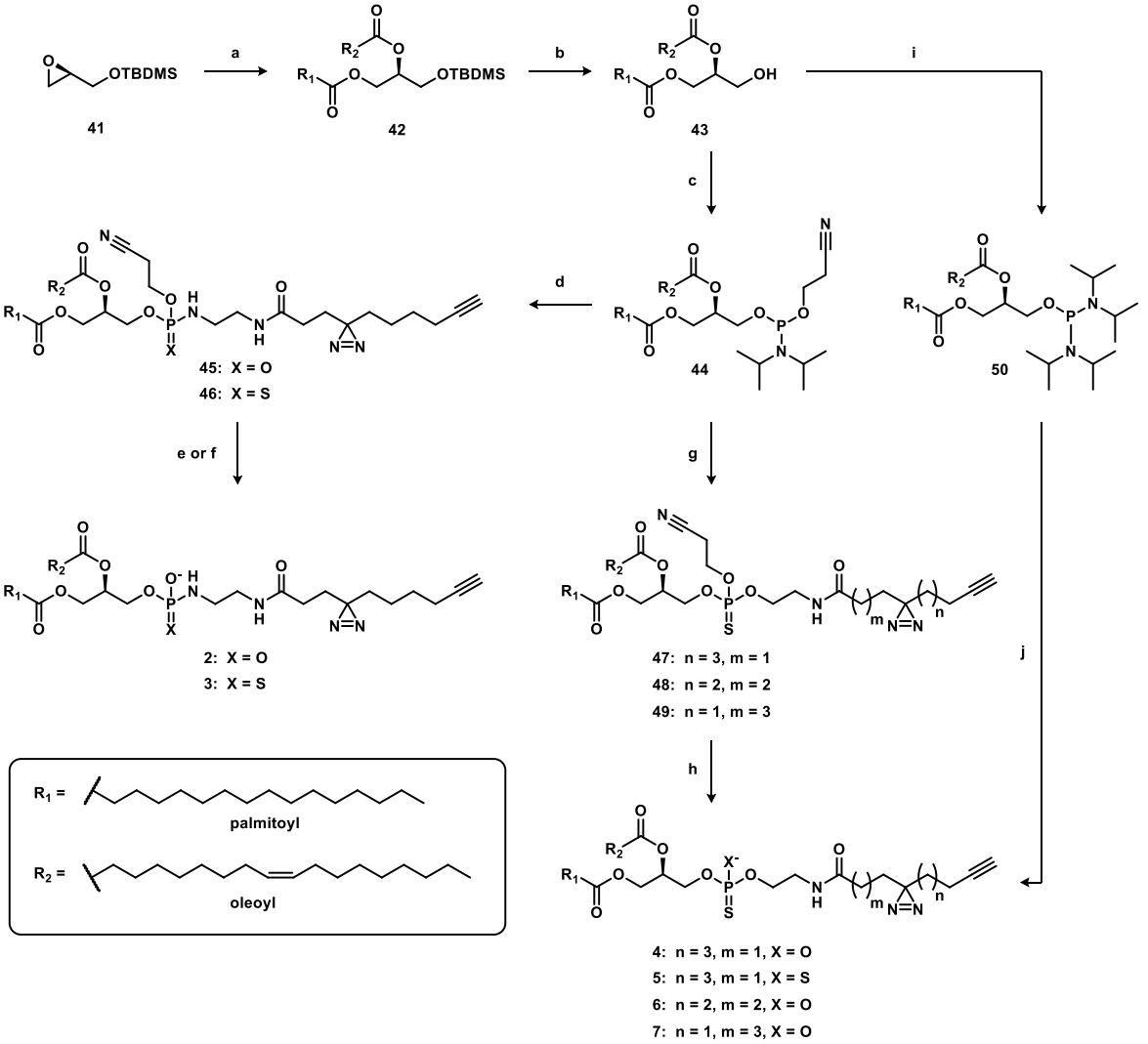


**Scheme 3.** Synthesis of photoprobes **2**-**7**. Reagents and conditions: a) *i.* palmitic acid, (*S*,*S*)-Co(salen), DiPEA, $O_2$; *ii*. oleic acid, DIC, DMAP, heptane, 0 °C to rt, 64%; b) $Et_3N{\cdot}3HF$, THF, $CH_3CN$, 99%; c) 2-cyanoethyl-*N*,*N*-diisopropylchlorophosphoramidite, DiPEA, DCM, 93%; d) *i.* for **45**: $H_2O$, 1*H*-tetrazole, $CH_3CN$; for **46**: $H_2S$, 1*H*-tetrazole, $CH_3CN$; *ii*. **37**, $CCl_4$, $Et_3N$, $CH_3CN$/DCM, 0 °C to rt, **45**: 80%, **46**: 31%; e) for **2**: **45**, DBU, DCM, 24%; f) for **3**: **46**, *t*-$BuNH_2$, DCM, 99%; g) *i*. **38**, **39** or **40**, 1*H*-tetrazole, DCM; *ii*. $S_8$, **47**: 59%, **48**: 42% **49**: 35%; h) *t*-$BuNH_2$, DCM, **4**: 81%, **6**: 21%, **7**: 25%; i) bis(diisopropylamino)chlorophosphine, DiPEA, DCM, 76%; j) for **5**: *i*. **38**, diisopropylammonium tetrazolide, DCM; *ii*. $H_2S$, 1*H*-tetrazole; *iii*. $Et_3N$, $S_8$, 7%.

Stabilized mono- and dithiophosphates were investigated as hydrolysis-resistant phosphodiester isosteres.[43-46] In addition, a potential favorable zinc-sulfur interaction was envisioned to increase enzyme affinity. Using phosphoramidite **44**, coupling with ethanolamides **38**-**40** and subsequent sulfurization with elemental sulfur gave protected monothiophosphates **47**-**49**. *tert*-Butylamine mediated deprotection afforded

thiophosphates **4**, **6** and **7** as a mixture of two diastereomers. For the dithiophosphate probe **5** an alternative route was investigated. Diacylglycerol **43** was transformed to phosphordiamidite **50**. To allow successful incorporation of both sulfur atoms, a three-step one-pot sequence was developed. This involved coupling of diamidite **50** with ethanolamide **38** using diisopropylammonium tetrazolide[47], affording the monosubstituted phosphoramidite. Of note, all attempts to couple with 1*H*-tetrazole resulted in disubstitution. Subsequently, the *in situ* generated monosubstituted phosphoramidite was converted to the *H*-thiophosphonate using hydrogen sulfide and finally sulfurized to obtain the desired dithiophosphate **5**.

### 4.2.2 Biological evaluation of NAPE-based photoprobes

The inhibitory activities of photoprobes **1**-**7** were assessed in the previously developed NAPE-PLD fluorescent substrate assay (Chapter 2). All compounds showed inhibitory activity for NAPE-PLD with poor to modest potencies (Figure 4A-B). In particular, the thiophosphoramidate **3** and dithiophosphate **5** showed reasonable activity with a $K_i$ below 10 μM. Next, the photoaffinity labeling properties of the photoprobes were evaluated in human embryonic kidney (HEK293T) cells. The probes (20 μM) were incubated with the cells for 30 minutes, irradiated with 350 nm UV light for 10 minutes, lysed, clicked with a Cy5-$N_3$ fluorophore and resolved by sodium dodecyl sulfate polyacrylamide gel electrophoresis (SDS-PAGE). Visualization by in-gel fluorescence scanning showed a UV-dependent protein labeling pattern (Figure 5). From this gel it was apparent that the thiophosphoramidate probe **3** was most effective in photocrosslinking various proteins. In

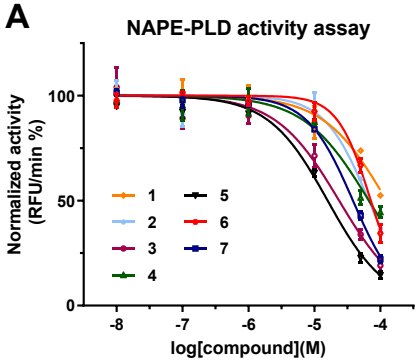


B

| ID | $pIC_{50}$ ± SEM | $K_i$ (μM) |
|---|---|---|
| **1** | 3.95 ± 0.08 | 42.1 |
| **2** | 4.13 ± 0.05 | 27.2 |
| **3** | 4.59 ± 0.06 | 9.4 |
| **4** | 4.15 ± 0.05 | 26.1 |
| **5** | 4.74 ± 0.05 | 6.8 |
| **6** | 4.10 ± 0.05 | 29.7 |
| **7** | 4.37 ± 0.03 | 15.8 |

**Figure 4.** NAPE-PLD inhibitory activities of NAPE-like photoprobes **1**-**7. A**) Dose response curves. **B**) $pIC_{50}$ and $K_i$ values. Data represent mean values ± SEM (N = 2, n = 2).

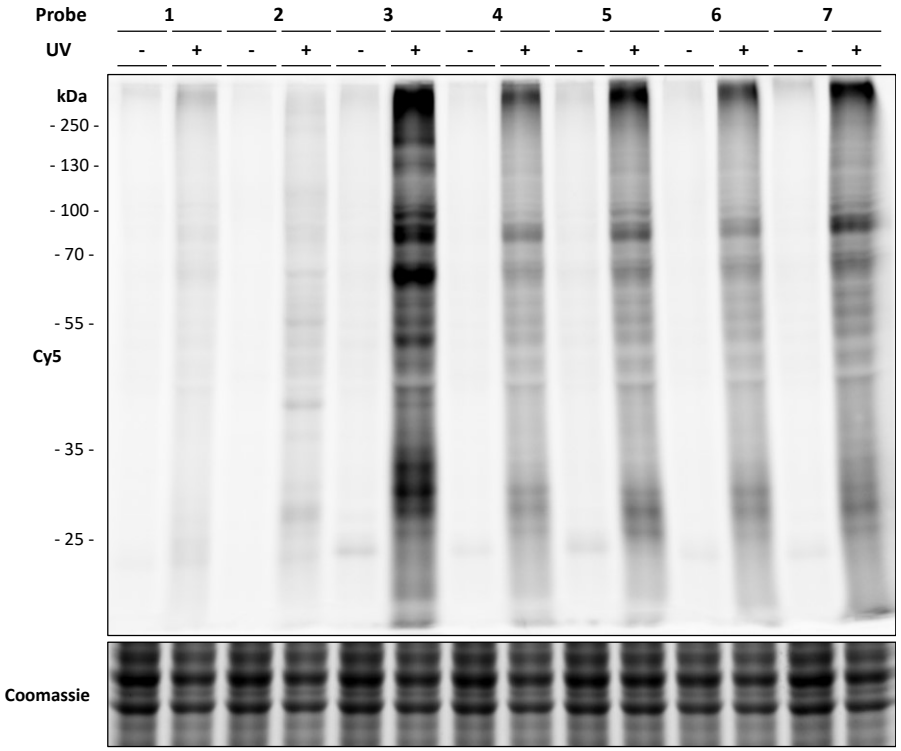


**Figure 5.** Photoaffinity labeling of NAPE-based photoprobes **1-7** (20 μM) shows UV-dependent labeling of proteins in live HEK293T cells. Coomassie was used as a protein loading control.

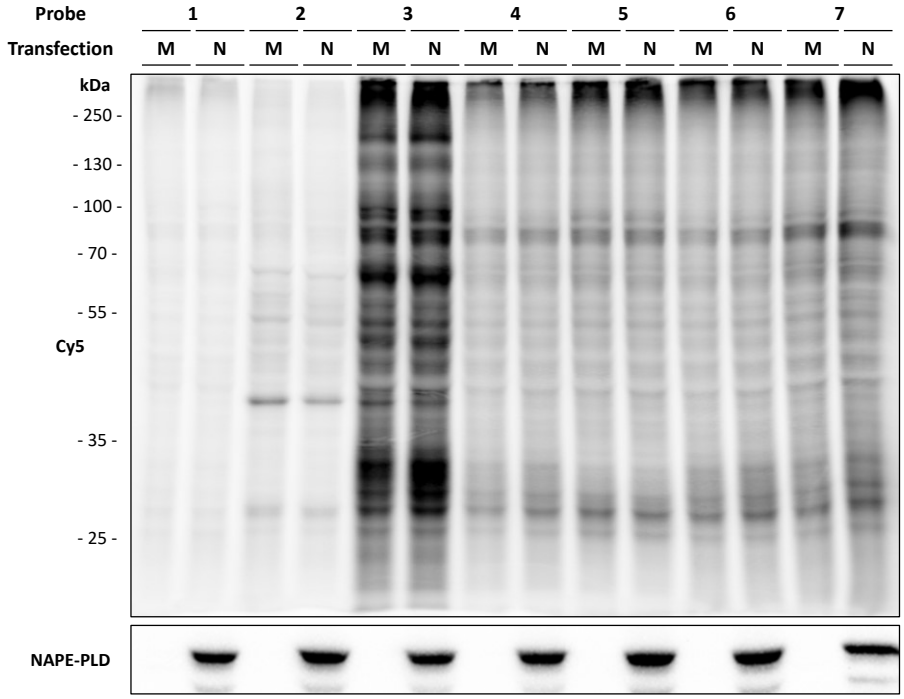


**Figure 6.** Live cell photoaffinity labeling of mock (M) and hNAPE-PLD (N) transfected HEK293T cells with NAPE-based photoprobes **1-7**. No labeling of NAPE-PLD was apparent at the expected height of 46 kDa (upper panel). Overexpression of hNAPE-PLD is confirmed in the western blot (lower panel).

contrast, probes **1** and **2** showed far less protein labeling, possibly due to their more labile phosphoramidate group or hydrolysis of the alkyne-containing acyl moiety.[42] The different mono- and dithiophosphate probes **4-7** exhibited similar labeling intensities and protein patterns. Furthermore, the position of the diazirine (probes **4**, **6** and **7**) did not appear to influence the labeling profile. To establish whether the photoprobes could visualize NAPE-PLD, HEK293T cells were overexpressed with human NAPE-PLD. 48 hours after transient transfection with a mock or hNAPE-PLD-FLAG containing pcDNA3.1 plasmid, the cells were treated with the different probes (20 μM) for 30 minutes. No band was visible at the expected height of hNAPE-PLD (46 kDa) for any of the photoprobes (Figure 6), indicating that these compounds were not capable of labeling NAPE-PLD.

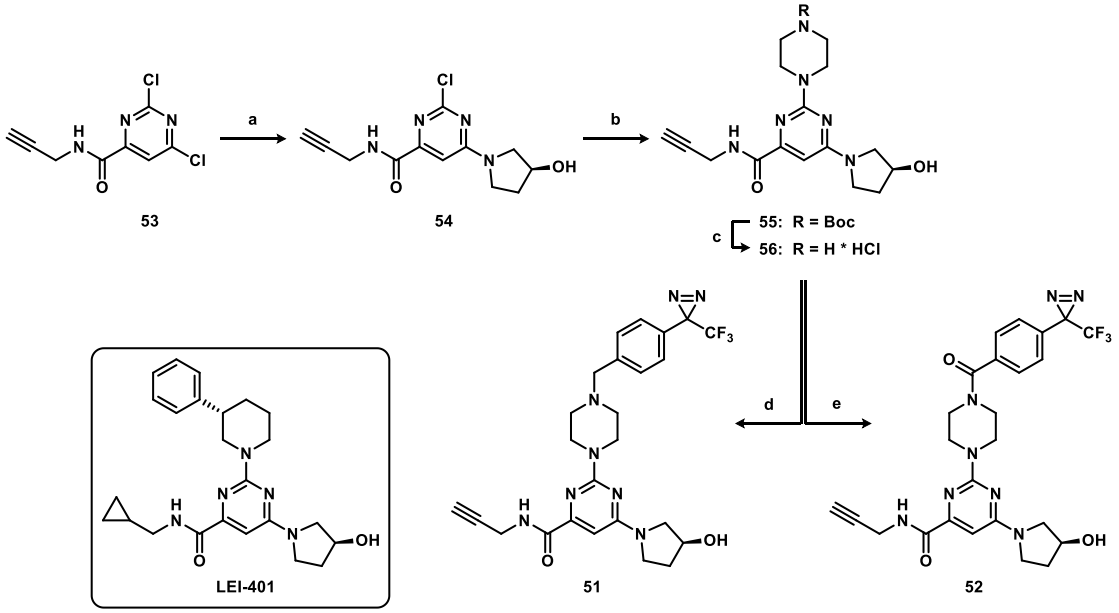


**Scheme 4.** Synthesis of photoprobes **51** and **52**. Reagents and conditions: a) (*S*)-3-hydroxypyrrolidine·HCl, DiPEA, MeOH, 0 °C, 83%; b) *N*-Boc-piperazine, DiPEA, *n*-BuOH, 100 °C, 90%; c) 4 M HCl, 1,4-dioxane, quant.; d) 4-(3-(trifluoromethyl)-3*H*-diazirin-3-yl)benzyl bromide, DiPEA, $CH_3CN$, 32%; e) 4-(3-(trifluoromethyl)-3*H*-diazirin-3-yl)benzoic acid, PyBOP, DiPEA, DMF, 0 °C to rt, 18%.

### 4.2.3 Synthesis of LEI-401-based photoprobes

**LEI-401** pyrimidine-6-carboxamide derivatives were explored as PAL probes, since this inhibitor series was developed to have optimal inhibitory activity towards NAPE-PLD and favorable physicochemical properties. Using the structure activity relationship map described in Chapter 3, photoprobes **51** and **52** were designed (Scheme 4). The

3-phenylpiperidine was substituted for a (trifluoromethyl-diazirine)benzyl- or benzoyl-piperazine as a photoreactive group. Replacement of the cyclopropylmethyl moiety for a propargyl group allowed introduction of reporter groups using click chemistry. Synthesis of probes **51** and **52** started with regioselective substitution of the dichloropyrimidine **53** (synthesis described in Chapter 3) with (*S*)-3-hydroxypyrrolidine to afford chloropyrimidine **54**. Nucleophilic aromatic substitution with *N*-Boc-piperazine followed by Boc deprotection furnished **56**. This compound was alkylated with 4-(3-(trifluoromethyl)-3*H*-diazirin-3-yl)benzyl bromide or condensed with 4-(3-(trifluoromethyl)-3*H*-diazirin-3-yl)benzoic acid, affording probes **51** and **52**, respectively.

### 4.2.4 Biological evaluation photoprobe 51 and 52.

The inhibitory activities of photoprobes **51** and **52** for hNAPE-PLD were measured in the PED6 assay, affording comparable submicromolar $K_i$ values (Figure 7A-B). Both probes showed a more than 30-fold increase in activity compared to the most potent NAPE-based photoactivatable probe **5**. In addition, due to their reduced lipophilicity, compounds **51** and **52** exhibit similar or greater lipophilic efficiencies (LipE) than **LEI-401 (**Figure 7B).

**A**

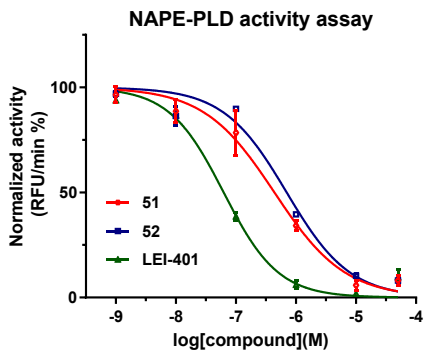


**B**

| ID | $pIC_{50}$ ± SEM | $K_i$ (µM) | cLogP[a] | LipE[b] |
|---|---|---|---|---|
| **LEI-401** | 7.14 ± 0.04 | 0.027 | 3.46 | 3.68 |
| **51** | 6.32 ± 0.07 | 0.18 | 2.66 | 3.66 |
| **52** | 6.21 ± 0.07 | 0.23 | 1.54 | 4.67 |

**Figure 7.** hNAPE-PLD inhibitory activities of pyrimidine-based photoprobes **51** and **52**. **A**) Dose response curves. **B**) $pIC_{50}$, $K_i$ values and physicochemical parameters. Data represent mean values ± SEM (N = 2, n = 2). [a] cLogP was calculated using Chemdraw 15; [b] Lipophilic efficiency (LipE) = $pIC_{50}$ – cLogP.

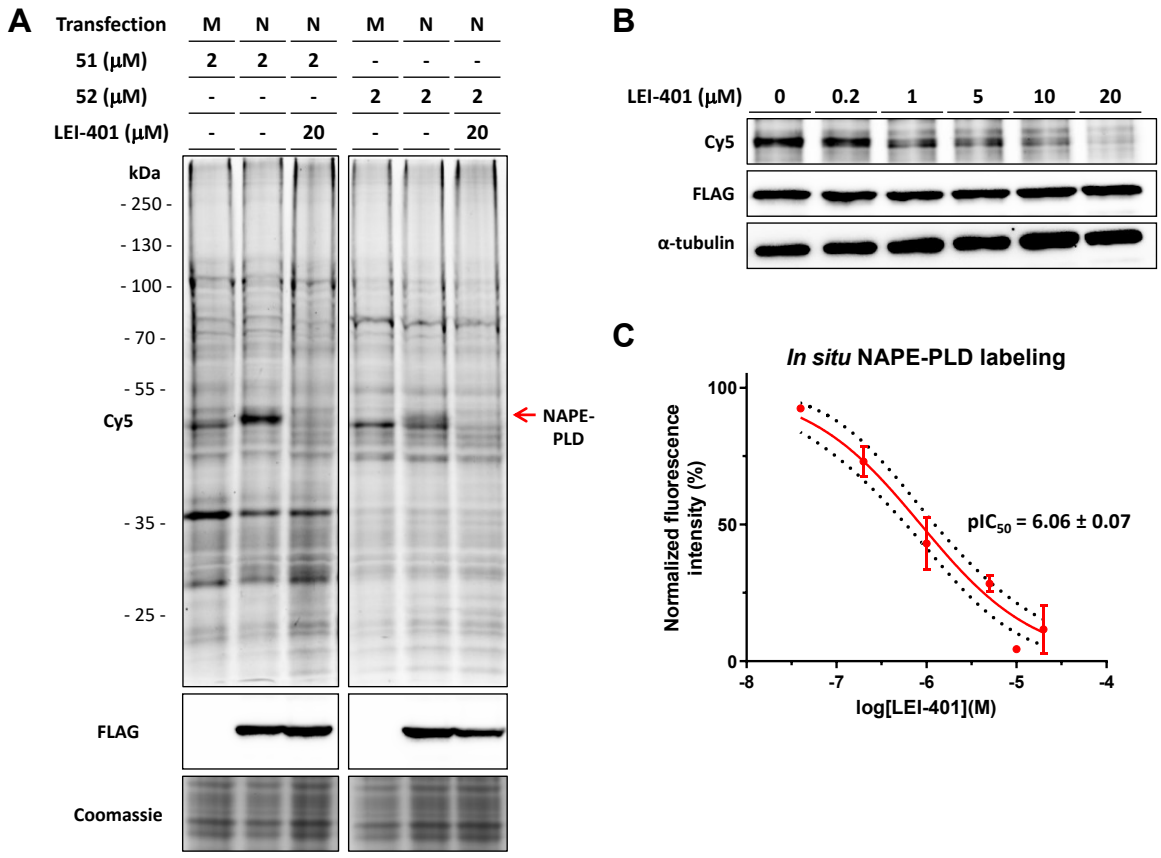


**Figure 8.** Photoprobes **51** and **52** enable visualization of NAPE-PLD in overexpressing HEK293T cells. **A**) Live cell photoaffinity labeling showing *in situ* fluorescent labeling of hNAPE-PLD-FLAG (N) at ~46 kDa in HEK293T cells but not in mock (M) transfected cells with probe **51** and **52** (2 μM) and displacement with **LEI-401** (20 μM) (upper panels). Anti-FLAG western blot displays expression of hNAPE-PLD-FLAG (lower panels). **B**) Representative gel of dose-dependent competition of probe **51** (2 μM) with **LEI-401**. **C**) Dose-response curve of **LEI-401** ($pIC_{50}$ = 6.06 ± 0.07, dotted lines show 95% confidence interval). Data represent mean values ± SEM for 3 biological replicates.

Probes **51** and **52** were also evaluated whether they could visualize NAPE-PLD in cells using the same experimental protocol as for the substrate-based probes. A fluorescent band at the expected molecular weight (MW) of ~46 kDa was apparent in the hNAPE-PLD transfected cells, but not in the control cells, for both probes. The fluorescent band overlapped with the FLAG-tag signal on western blot (Figure 8A, left and middle lanes). These results indicate that hNAPE-PLD can be successfully labeled by the inhibitor-based photoaffinity probes. Importantly, the intensity of the fluorescent band was reduced when co-incubated with **LEI-401** (20 μM), thereby confirming that **LEI-401** engaged with NAPE-PLD in living cells (Figure 8A, right lanes). Of note, a fluorescent band was observed at the same MW in the mock lanes that also could be competed out by **LEI-401**, which

may possibly indicate the presence of endogenous NAPE-PLD. Next, concentration response experiments were performed with probe **51**, as the labeling of this compound was more intense than **52**. **LEI-401** displayed a dose-dependent reduction of NAPE-PLD labeling, which was quantified as a cellular $IC_{50}$ of 0.86 μM (95% confidence interval (CI): 0.60 – 1.2 μM) (Figure 8B-C).

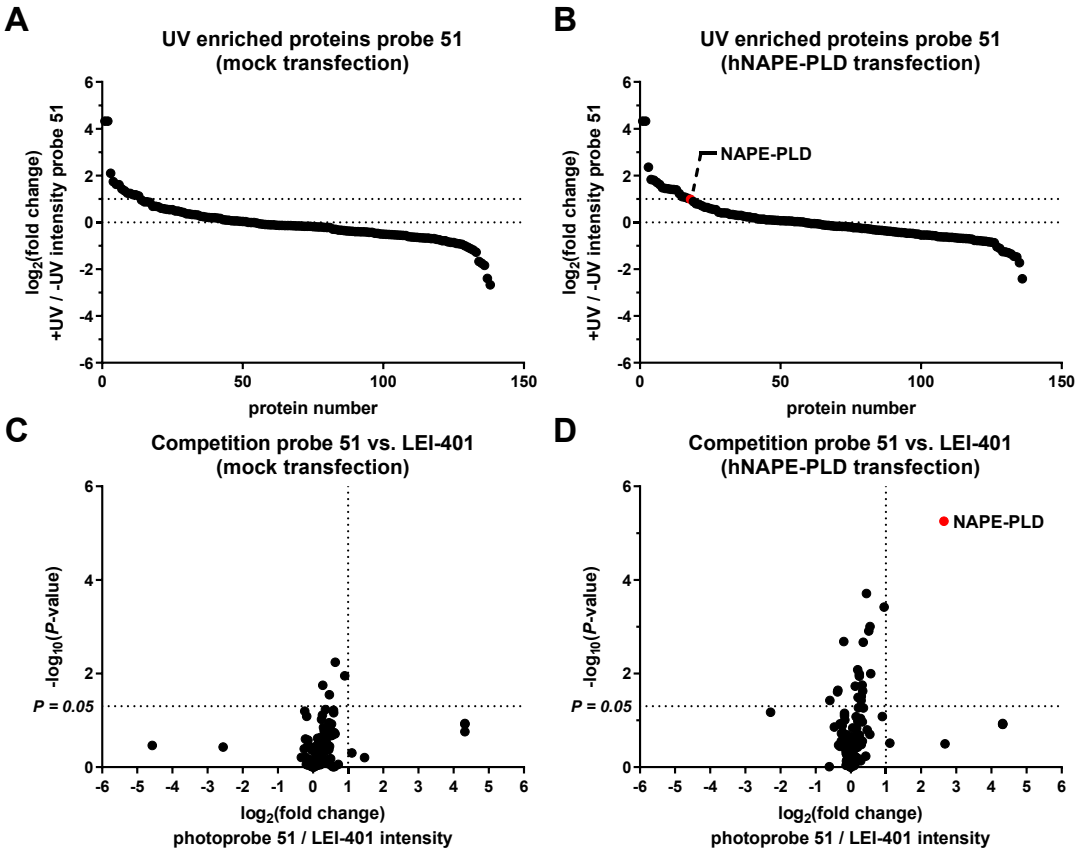


**Figure 9. A-B**) Waterfall plots showing UV enriched proteins of photoprobe **51** (2 μM) in HEK293T with mock or hNAPE-PLD-FLAG transfection. **C-D**) Volcano plots displaying competed protein targets for photoprobe **51** (2 μM) vs. **LEI-401** (20 μM) in mock (**C**) or hNAPE-PLD-FLAG (**D**) transfected HEK293T cells (3 biological replicates per condition). Cut-off values for protein target validation: unique peptides ≥ 2; UV enrichment: $\log_2$(fold change) > 1 (+UV/-UV **51** intensity); for competition: $\log_2$(fold change) > 1 (**51** intensity/**LEI-401** intensity). Statistically significant targets: $P < 0.05$ using Student's *t*-test (unpaired, two-tailed) and Benjamini-Hochberg correction with a false discovery rate (FDR) of 10%.

**Table 1.** Protein targets of photoprobe **51** in mock and hNAPE-PLD-FLAG transfected HEK293T cells.

| Name | Gene | MW (kDa) | Accession | Peptides | | $log_2$(ratio) | | | | *P*-value | | | |
|---|---|---|---|---|---|---|---|---|---|---|---|---|---|
| | | | | | | mock | | NAPE-PLD | | mock | | NAPE-PLD | |
| | | | | Total | Unique | +UV/ -UV | 51/ LEI-401 | +UV/ -UV | 51/ LEI-401 | +UV/ -UV | 51/ LEI-401 | +UV/ -UV | 51/ LEI-401 |
| ***N*-acylphosphatidyl-ethanolamine phospholipase D** | ***NAPEPLD*** | **46** | **Q6IQ20** | **8** | **6** | **-** | **-** | **0.99** | **2.65** | **-** | **-** | **>0.001** | **>0.001** |
| Epoxide hydrolase 1 | *EPHX1* | 53 | P07099 | 16 | 10 | 1.25 | 0.90 | 1.62 | 0.95 | 0.0023 | 0.0112 | >0.001 | >0.001 |
| Ras-related protein Rab-10 | *RAB10* | 23 | P61026 | 5 | 2 | 1.18 | 0.16 | 1.71 | 0.36 | 0.0056 | 0.2808 | 0.0032 | 0.0542 |
| Probable serine carboxypeptidase | *CPVL* | 54 | Q9H3G5 | 5 | 5 | 1.74 | 0.24 | 1.80 | 0.33 | >0.001 | 0.0956 | 0.0016 | 0.1077 |
| Lamin-B1 | *LMNB1* | 67 | P20700 | 14 | 13 | 2.10 | 0.18 | 2.36 | 0.06 | 0.0012 | 0.3413 | >0.001 | 0.6149 |
| Lamin-B2 | *LMNB2* | 70 | Q03252 | 8 | 6 | 4.32 | 0.13 | 4.32 | -0.01 | >0.001 | 0.4515 | >0.001 | 0.9016 |

Cut-off values for protein target validation: unique peptides ≥ 2, UV enrichment: $log_2$(fold change) ≥ 1 (UV+/UV- **51** intensity), for competition: $log_2$(fold change) ≥ 1 (**51** intensity/**LEI-401** intensity). Statistically significant targets: $P < 0.05$ using Student's *t*-test (unpaired, two-tailed) and Benjamini-Hochberg correction with FDR of 10%.

To unequivocally establish the identity of the labeled band and determine the selectivity of **LEI-401**, label-free chemical proteomics experiments were performed.[11] Cell lysates prepared from mock or hNAPE-PLD-HEK293T cells incubated and UV-irradiated with probe **51** (2 μM), were clicked with a biotin-$N_3$, which allowed for an enrichment of the probe-labeled proteins using avidin agarose beads, followed by trypsin digestion and protein identification by mass spectrometry. Proteomic analysis revealed that probe **51** interacted with 136 to 138 proteins (Figure 9A-B). NAPE-PLD was significantly enriched by probe **51** in a UV-dependent manner, exclusively in the hNAPE-PLD transfected cells (Figure 9B), and its labeling was prevented by co-incubation with **LEI-401** (20 μM) (Figure 9D). Besides NAPE-PLD, five endogenous protein targets were confirmed for probe **51** in both mock and NAPE-PLD overexpressing cells (Table 1). **LEI-401** did not compete with probe **51** for any of these proteins, indicating that **LEI-401** selectively engages with NAPE-PLD over the other targets of **51** in HEK293T cells (Figure 9C-D).

## 4.3 Discussion

In this chapter, two strategies were explored for the development of NAPE-PLD PAL probes. Seven synthetically challenging NAPE-based photoprobes were produced, incorporating various phosphodiester bioisosteres. Probes **1**-**7** did not exhibit high affinity for NAPE-PLD and, as a result, were unable to visualize NAPE-PLD in live cell gel experiments. The second design was based on the potent NAPE-PLD inhibitor **LEI-401**, which yielded photoactivatable probes **51** and **52**. These probes exhibited several advantages compared to the NAPE-based compounds, including increased inhibitory activity for NAPE-PLD, a more efficient photocrosslinking group and improved physicochemical parameters thereby enhancing solubility and cell-permeability. In particular, probe **51** showed efficient photolabeling of NAPE-PLD in live overexpressing HEK293T cells, which could be competed out by co-incubation with **LEI-401**. Chemical proteomics was used to confirm the identity of NAPE-PLD, thereby providing evidence that **LEI-401** binds with its intended target in a cellular system.

Visualization of endogenous NAPE-PLD is highly valuable to study its biological role in cells. Although a band was apparent in the mock transfected HEK293T cells for both probes **51** and **52** which could be competed out by **LEI-401**, no endogenous NAPE-PLD was observed in the proteomics experiments for these samples. Also in mouse neuroblastoma Neuro2A cells which express NAPE-PLD, probes **51** and **52** were not able to label NAPE-PLD (data not shown). Possible explanations include low efficiency of photocrosslinking, inherent to photoaffinity labeling, as well as technical limitations with regard to

measuring low abundant NAPE-PLD peptides. Discrepancies between the efficiency of the click reaction with Cy5-$N_3$ or biotin-$N_3$ have to be taken into account as well. Further optimizations to enable endogenous NAPE-PLD labeling could consist of increasing the NAPE-PLD affinity of the probes or adjusting the position of the photocrosslinker. Alternatively, increasing endogenous NAPE-PLD expression could be used to obtain effective labeling, although so far, no such agents have been identified.

To conclude, the development of photoaffinity probe **51** and **52** enabled the detection of NAPE-PLD in living cells and its target engagement by **LEI-401**. Photoprobes **51** and **52** in combination with **LEI-401** therefore expand the currently available toolbox for studying NAPE-PLD and anandamide biology in cellular models.

## Acknowledgements

Rob Bosman, Branca van Veen and Jasper van de Sande are kindly acknowledged for contributing to the compound synthesis and biochemical testing. Bobby Florea and Alexander Bakker are kindly acknowledged for performing proteomics measurements.

## 4.4 Experimental Section

### A. Biological procedures

**NAPE-PLD surrogate substrate activity assay**

The NAPE-PLD activity assay was performed as described in Chapter 2.

**Cloning of plasmid DNA**

Full length human cDNA of human NAPE-PLD (obtained from Natsuo Ueda[34]) was cloned into mammalian expression vector pcDNA3.1, containing a C-terminal FLAG-tag and genes for ampicillin and neomycin resistance. All plasmids were grown in XL-10 Z-competent cells and prepped (Maxi Prep, Qiagen). Constructs were verified by Sanger sequencing (Macrogen).

**Cell culture**

HEK293T cells (ATCC) were cultured at 37 $^{o}$C and 7% $CO_2$ in DMEM (Sigma Aldrich, D6546) with GlutaMax (2 mM), penicillin (100 μg/ml), streptomycin (100 μg/ml) and 10% fetal calf serum. Cells were passaged twice a week to appropriate confluence by thorough pipetting.

**Gel-based photoaffinity labeling**

500,000 HEK293T cells per well were seeded in a 12-well plate 1 day before transfection. On the day of transfection the medium was refreshed with 0.375 mL medium per well. Transfection was performed with polyethyleneimine (PEI, 3 μg per well) and human NAPE-PLD or Mock pcDNA3.1Neo plasmids (1 μg per well). PEI and plasmids were combined in serum-free medium (0.125 mL per well) and incubated for 15 min at rt, then added to each well. After 24 h the medium was refreshed. 48 hours after transfection the

medium was removed and cells were washed with warm PBS (1x). This was followed by treatment with the photoprobes **1**-**7** (1000x in DMSO, final concentration: 20 μM) or photoprobes **51**-**52** (1000x in DMSO, final concentration: 2 μM) together with vehicle or competitor (600x in DMSO) in medium + serum (0.30 mL per well) for 30 min at 37 °C. The medium was aspirated and the cells were covered with PBS (0.15 mL per well), followed by 350 nm UV irradiation using a Caprobox™ at 4 °C for 10 min. The cells were harvested into 1.5 mL epps with cold PBS and centrifuged for 10 min at 2000 rpm at 4 °C. The PBS was removed and the cells were flash frozen with liquid $N_2$ (cells can optionally be stored at -80 °C). The cells were lysed with lysis buffer (30 μL, 20 mM HEPES pH 7.2, 0.25 M sucrose, 1 mM $MgCl_2$, benzonase 25 U/mL) followed by pipetting up and down and incubating for 30 min on ice. Protein concentrations were measured using a Bradford assay (Bio-Rad), and cell lysates were diluted to 2 μg/μL with lysis buffer. 18 μg cell lysate (9 μL) was then clicked with Cy5-$N_3$ (for molecular structure see Figure S2) using a click mix (1 μL per sample, final concentrations: 1 mM $CuSO_4$, 6 mM sodium ascorbate, 0.2 mM tris(3-hydroxypropyltriazolylmethyl)-amine (THPTA), 2 μM Cy5-$N_3$) for 1 h at rt (Note: it is important to separately prepare the click mix first with $CuSO_4$ and sodium ascorbate, until a yellow color change is observed). Samples were denatured with 4x Laemmli buffer (3.33 μL, stock concentration: 240 mM Tris-HCl pH 6.8, 8% w/v SDS, 40% v/v glycerol, 5% v/v β-mercaptoethanol, 0.04% v/v bromophenol blue) and incubated for 30 min at rt. The samples were resolved by SDS-PAGE (10% acrylamide gel) at 180 V for 75 min, after which the gels were imaged at Cy3 and Cy5 channels (605/50 and 695/55 filters, respectively) on a ChemiDoc™ Imaging System (Bio-Rad). Fluorescence is normalized to Coomassie or α-tubulin by western blot using ImageLab software (Bio-Rad). $IC_{50}$ curves were generated using Graphpad Prism v6.

**Western blot**

Proteins were transferred from the resolved SDS-PAGE gel to a 0.2 μm PVDF membrane using a Trans-Blot® Turbo (Bio-Rad). The membranes were washed with TBS (50 mM Tris-HCl pH 7.5, 150 mM NaCl) and blocked with 5% milk in TBST (50 mM Tris-HCl pH 7.5, 150 mM NaCl, 0.05% Tween 20) 1 h at rt or overnight at 4 °C. Primary antibodies against NAPE-PLD (Abcam, ab95397, 1:200, in TBST), FLAG-tagged proteins (Sigma Aldrich, F3165, 1:5000 in 5% milk in TBST) or α-tubulin (Genetex, GTX76511, 1:5000 in 5% milk in TBST) were incubated 1 h at rt or overnight at 4 °C. Membranes were washed with TBST and incubated with secondary antibodies: for NAPE-PLD, goat-anti-rabbit-HRP (Santa Cruz, sc-2030, 1:2000 in 5% milk in TBST); for FLAG-tagged proteins, goat-anti-mouse-HRP (Santa Cruz, sc-2005, 1:5000 in 5% milk in TBST); for α-tubulin, goat-anti-rat (Santa Cruz, sc-2032, 1:5000 in 5% milk in TBST). All secondary antibodies were incubated or 1 h at rt. Membranes were washed with TBST and TBS. The blot was developed in the dark using a luminol solution (10 mL, 1.4 mM luminol in Tris-HCl pH 7.5), ECL enhancer (100 μL, 6.7 mM *para*-hydroxycoumaric acid in DMSO) and $H_2O_2$ (3 μL, 30% w/w in $H_2O$). Chemiluminescence was visualized using a ChemiDoc™ Imaging System (Bio-Rad). Band intensity is normalized to α-tubulin using ImageLab software (Bio-Rad).

**Chemical proteomics-based photoaffinity labeling**

$2 \cdot 10^6$ HEK293T cells per well were seeded in a 6-well plate 1 day before transfection. On the day of transfection the medium was removed and refreshed with 1.125 mL fresh medium per well. Transfection was performed with polyethyleneimine (PEI, 9 μg per well) and human NAPE-PLD or Mock pcDNA3.1Neo plasmids (3 μg per well). PEI and plasmids were combined in serum-free medium (0.375 mL per well) and incubated for 15 min at rt, then added to each well. After 24 h the medium was refreshed. 48 hours after transfection the medium was removed and cells were washed with warm PBS (1x). This was followed by treatment with photoprobe **51** (1000x in DMSO, final concentration: 2 μM) together with vehicle or competitor (1000x in DMSO, final concentration: 20 μM) in medium + serum (1 mL per well) for 30 min at 37 °C. The medium was aspirated and the cells were covered with PBS (0.5 mL per well), followed by 350 nm UV irradiation using a Caprobox™ at 4 °C for 10 min. The cells were harvested into 1.5 mL epps with cold PBS and centrifuged for 10 min at 2000 rpm at 4 °C. The PBS was removed and the cells were flash frozen with

liquid $N_2$ (cells can optionally be stored at -80 °C). The cells were lysed with lysis buffer (30 μL, 20 mM HEPES pH 7.2, 0.25 M sucrose, 1 mM $MgCl_2$, benzonase 25 U/mL) followed by pipetting up and down and incubating for 30 min on ice. Protein concentrations were measured using a Bradford assay (Bio-Rad), and cell lysates were diluted to 1 μg/μL with lysis buffer.

From here the label-free chemical proteomics protocol was followed as previously described.[11] 270 μg cell lysate (270 μL) was clicked with biotin-$N_3$ (Sigma Aldrich, 762024) using a click mix (30 μL per sample, final concentrations: 1 mM $CuSO_4$, 6 mM sodium ascorbate, 0.2 mM tris(3-hydroxypropyltriazolylmethyl)amine (THPTA), 4 μM biotin-$N_3$) for 1 h at rt (Note: it is important to separately prepare the click mix first with CuSO4 and sodium ascorbate, until a yellow color change is observed). Proteins were precipitated using chloroform (166 μL), methanol (666 μL) and MilliQ (366 μL). Samples were centrifuged for 10 min at 1500 g and the solvents were carefully removed. Methanol (600 μL) was added and the proteins were resuspended using a probe sonicator (30% amplitude, 10 s). After centrifugation (5 min, 18,400 g) the supernatant was removed and the samples were resuspended again in urea buffer (250 μL, 6 M urea, 250 mM $NH_4HCO_3$) by pipetting up and down. DTT (2.5 μL, final concentration 10 mM) was added and the samples were incubated at 65 °C with shaking (600 rpm) for 15 min. After cooling to rt, iodoacetamide (20 μL, final concentration 40 mM) was added and incubated in the dark at 20 °C with shaking (600 rpm) for 30 min. Next, SDS (70 μL, 10%) was added and incubated at 65 °C with shaking (600 rpm) for 5 min. For 18 samples, 1.8 mL of avidin agarose beads (Thermo Scientific, 20219) were divided over three 15 mL tubes and washed with PBS (3 x 10 mL). The beads in each tube were resuspended in PBS (6 mL) and divided over 18 tubes (1 mL each). To each tube was added the denatured sample and PBS (2 mL) and the tubes were rotated with an overhead shaker at rt for 3 h. After centrifugation (2 min, 2,500 g) and removal of the supernatant, the beads were consecutively washed with 0.5% SDS in PBS (w/v, 6 mL) and PBS (3 x 6 mL), each time centrifuging (2 min, 2,500 g). The beads were transferred to a 1.5 mL low binding epp (Sarstedt, 72.706.600) with on-bead digestion buffer (250 μL, 100 mM Tris pH 8.0, 100 mM NaCl, 1 mM $CaCl_2$, 2% v/v acetonitrile) and to each sample was added 1 μL trypsin solution (0.5 μg/μL trypsin (Promega, V5111), 0.1 mM HCl). Proteins were digested at 37 °C with shaking (950 rpm) overnight. Formic acid (12.5 μL) was added to each sample and the beads were filtered off using a biospin column (Bio-Rad, 7326204), the flow-through was collected in a 2 mL epp. Samples were purified using StageTips[48]. Each StageTip was conditioned with MeOH (50 μL, centrifugation: 2 min, 300 g), followed by StageTip solution B (50 μL, 80% v/v acetonitrile, 0.5% v/v formic acid in MilliQ, centrifugation: 2 min, 300 g) and StageTip solution A (50 μL, 0.5% v/v formic acid in MilliQ, centrifugation: 2 min, 300 g). Next, the samples were loaded, centrifuged (2 min, 600 g) and the peptides on the StageTip were washed with StageTip solution A (100 μL, centrifugation: 2 min, 600 g). The StageTips were transferred to a new 1.5 mL low binding epp and the peptides were eluted with StageTip solution B (100 μL, centrifugation: 2 min, 600 g). The solvents were evaporated to dryness in a SpeedVac concentrator at 45 °C for 3 h. Samples were reconstituted in LC-MS solution (50 μL, 3% v/v acetonitrile, 0.1% v/v formic acid, 1 μM yeast enolase peptide digest (Waters, 186002325) in MilliQ).

The peptides were measured as described previously for the NanoACQUITY UPLC System coupled to SYNAPT G2-Si high definition mass spectrometer.[11] A trap-elute protocol, where 5 μL of the digest is loaded on a trap column (C18 100 Å, 5 μM, 180 μM x 20 mm, Waters) followed by elution and separation on the analytical column (HSS-T3 C18 1.8 μM, 75 μM x 250 mm, Waters). The sample is brought onto this column at a flow rate of 10 μL/min with 99.5% solvent A for 2 min before switching to the analytical column. Peptide separation is achieved using a multistep concave gradient based on gradients previously described.[49] The column is re-equilibrated to initial conditions after washing with 90% solvent B. The rear seals of the pump are flushed every 30 min with 10% (v/v) acetonitrile. [Glu1]-fibrinopeptide B (GluFib) is used as a lock mass compound. The auxiliary pump of the LC system is used to deliver this peptide to the reference sprayer (0.2 μL/min). A UDMSe method is set up as previously described.[49] Briefly, the mass range is set from 50 to 2,000 Da with a scan time of 0.6 seconds in positive, resolution mode. The collision energy is set to 4 V in the trap cell for low-energy MS mode. For the elevated energy scan, the transfer cell collision energy is ramped using

drift-time specific collision energies. The lock mass is sampled every 30 seconds. For raw data processing, PLGS (v3.0.3) was used. The $MS^E$ identification workflow was performed with the parameters summarized in Table S1 to search the human proteome from Uniprot (uniprot-homo-sapiens-trypsin-reviewed-2016_08_29.fasta). Protein quantification was performed using ISOQuant (v1.5). The parameter settings used are summarized in Table S2.

**Table S1.** The PLGS parameter settings used

| Parameter | Value |
|---|---|
| Lock mass m/z | 785.8426 |
| Low energy threshold | 150 counts |
| Elevated energy threshold | 30 counts |
| Digest reagent | trypsin |
| Max missed cleavages | 2 |
| Modifications | Fixed carbamidomethyl C, variable oxidation M |
| FDR less than | 1% |
| Fragments/peptide | 2 |
| Fragments/protein | 5 |
| Peptides/protein | 1 |

**Table S2.** ISOQuant parameter settings used

| Parameter | Value |
|---|---|
| isoquant.pluginQueue.name | design project and run ISOQuant analysis |
| process.peptide.deplete.PEP_FRAG_2 | false |
| process.peptide.deplete.CURATED_0 | false |
| process.peptide.statistics.doSequenceSearch | false |
| process.emrt.minIntensity | 1000 |
| process.emrt.minMass | 500 |
| process.emrt.rt.alignment.match.maxDeltaMass.ppm | 10 |
| process.emrt.rt.alignment.match.maxDeltaDriftTime | 2 |
| process.emrt.rt.alignment.normalizeReferenceTime | false |
| process.emrt.rt.alignment.maxProcesses | 24 |
| process.emrt.rt.alignment.referenceRun.selectionMethod | AUTO |
| process.emrt.clustering.preclustering.orderSequence | MTMTMT |
| process.emrt.clustering.preclustering.maxDistance.mass.ppm | 6.06E-6 |
| process.emrt.clustering.preclustering.maxDistance.time.min | 0.202 |
| process.emrt.clustering.preclustering.maxDistance.drift | 2.02 |
| process.emrt.clustering.distance.unit.mass.ppm | 6.0E-6 |
| process.emrt.clustering.distance.unit.time.min | 0.2 |
| process.emrt.clustering.distance.unit.drift.bin | 2 |
| process.emrt.clustering.dbscan.minNeighborCount | 1 |

| | |
|---|---|
| process.identification.peptide.minReplicationRate | 2 |
| process.identification.peptide.minScore | 5.5 |
| process.identification.peptide.minOverallMaxScore | 5.5 |
| process.identification.peptide.minSequenceLength | 6 |
| process.identification.peptide.acceptType.PEP_FRAG_1 | true |
| process.identification.peptide.acceptType.IN_SOURCE | false |
| process.identification.peptide.acceptType.MISSING_CLEAVAGE | false |
| process.identification.peptide.acceptType.NEUTRAL_LOSS_H20 | false |
| process.identification.peptide.acceptType.NEUTRAL_LOSS_NH3 | false |
| process.identification.peptide.acceptType.PEP_FRAG_2 | true |
| process.identification.peptide.acceptType.DDA | true |
| process.identification.peptide.acceptType.VAR_MOD | true |
| process.identification.peptide.acceptType.PTM | true |
| process.annotation.peptide.maxSequencesPerEMRTCluster | 1 |
| process.annotation.protein.resolveHomology | true |
| process.annotation.peptide.maxFDR | 0.01 |
| process.annotation.useSharedPeptides | all |
| process.normalization.lowess.bandwidth | 0.3 |
| process.normalization.orderSequence | XPIR |
| process.normalization.minIntensity | 3000 |
| process.quantification.peptide.minMaxScorePerCluster | 5.5 |
| process.quantification.peptide.acceptType.IN_SOURCE | false |
| process.quantification.peptide.acceptType.MISSING_CLEAVAGE | false |
| process.quantification.peptide.acceptType.NEUTRAL_LOSS_H20 | false |
| process.quantification.peptide.acceptType.NEUTRAL_LOSS_NH3 | false |
| process.quantification.peptide.acceptType.PEP_FRAG_1 | true |
| process.quantification.peptide.acceptType.PEP_FRAG_2 | false |
| process.quantification.peptide.acceptType.VAR_MOD | false |
| process.quantification.peptide.acceptType.PTM | false |
| process.quantification.peptide.acceptType.DDA | true |
| process.quantification.topx.degree | 3 |
| process.quantification.topx.allowDifferentPeptides | true |
| process.quantification.minPeptidesPerProtein | 2 |
| process.quantification.absolute.standard.entry | ENO1_YEAST |
| process.quantification.absolute.standard.fmol | 50 |
| process.quantification.topx.allowDifferentPeptides | true |
| process.quantification.absolute.standard.entry | ENO1_YEAST |
| process.quantification.absolute.standard.fmol | 50 |
| process.quantification.maxProteinFDR | 0.01 |

**Data analysis**

Protein targets of photoprobe **51** were selected based on the following cut-offs: 1) ≥ 2-fold enrichment for UV-treated vs. non-UV-treated samples; 2) unique peptides ≥ 2; 3) testing for significance using Student's *t*-test (unpaired, two-tailed), $P < 0.05$ is considered significant; 4) Benjamini–Hochberg correction with an false discovery rate (FDR) of 10%.

## B. Synthetic procedures

**General**

All chemicals (Sigma-Aldrich, Fluka, Acros, Merck, Combi-Blocks, Fluorochem, TCI) were used as received. All solvents used for reactions were of analytical grade. THF, $Et_2O$, DMF, $CH_3CN$ and DCM were dried over activated 4 Å molecular sieves, MeOH over 3 Å molecular sieves. Flash chromatography was performed on silica gel (Screening Devices BV, 40-63 μm, 60 Å). The eluent EtOAc was of technical grade and distilled before use. Reactions were monitored by thin layer chromatography (TLC) analysis using Merck aluminium sheets (Silica gel 60, $F_{254}$). Compounds were visualized by UV-absorption (254 nm) and spraying for general compounds: $KMnO_4$ (20 g/L) and $K_2CO_3$ (10 g/L) in water, or for amines: ninhydrin (0.75 g/L) and acetic acid (12.5 mL/L) in ethanol, followed by charring at ~150 $^oC$. $^1H$, $^{13}C$ and $^{31}P$ NMR experiments were recorded on a Bruker AV-300 (300/75 MHz), Bruker AV-400 (400/101/162 MHz), Bruker DMX-400 (400/101/162 MHz), Bruker AV-500 (500/126/202 MHz) and Bruker AV-600 (600/151 MHz). Chemical shifts are given in ppm (δ) relative to tetramethylsilane or $CDCl_3$ as internal standards. Multiplicity: s = singlet, br s = broad singlet, d = doublet, dd = doublet of doublet, t = triplet, q = quartet, p = pentet, m = multiplet. Coupling constants (*J*) are given in Hz. LC-MS measurements were performed on a Thermo Finnigan LCQ Advantage MAX ion-trap mass spectrometer ($ESI^+$) coupled to a Surveyor HPLC system (Thermo Finnigan) equipped with a standard C18 (Gemini, 4.6 mm D x 50 mm L, 5 μm particle size, Phenomenex) analytical column and buffers A: $H_2O$, B: $CH_3CN$, C: 0.1% aq. TFA. High resolution mass spectra were recorded on a LTQ Orbitrap (Thermo Finnigan) mass spectrometer or a Synapt G2-Si high definition mass spectrometer (Waters) equipped with an electrospray ion source in positive mode (source voltage 3.5 kV, sheath gas flow 10 mL min-1, capillary temperature 250 $^oC$) with resolution R = 60000 at m/z 400 (mass range m/z = 150-2000) and dioctylphtalate (m/z = 391.28428) as a lock mass. Preparative HPLC was performed on a Waters Acquity Ultra Performance LC with a C18 column (Gemini, 150 x 21.2 mm, Phenomenex). All final compounds were determined to be > 95% pure by integrating UV intensity recorded via HPLC.

**Important experimental note**

***Trace metal chelation:*** the phosphothioate and phosphordithioate moieties are known to chelate trace metals. High purity grade silica gel (Sigma-Aldrich, Davisil Grade 633) should be used for the purification of these compounds. The silica gel can be regenerated after use by flushing with MeOH (4 CV) and $Et_2O$ (2 CV), followed by drying in a vacuum stove at 100 $^oC$. In the case of metal chelation, strong peak broadening was observed by $^{31}P$-NMR. This could be reversed by dissolving the compound in 10% MeOH in $CHCl_3$, adding an excess of EDTA-disodium in MilliQ and stirring for 30 min. The $^{31}P$-NMR peak intensity could be recovered, after which the aqueous layer was separated, the organic layer was washed with MilliQ and the solvents were concentrated under reduced pressure.

**General procedure A**

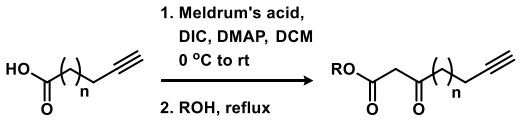


A round bottom flask was charged with the fatty acid (1 eq) and dry DCM (0.5 M) and cooled to 0 °C. Meldrum's acid (1.1 eq) and DMAP (1.2 – 1.3 eq) were added. This was followed by dropwise addition of a DIC solution (1.2 – 1.3 eq) in DCM (2 M) over 30 min, giving a yellow solution. The reaction was warmed to rt and stirred for 3 h. The mixture was diluted with DCM and washed with 1 M aq. $KHSO_4$ (2x), brine (1x), dried ($Na_2SO_4$), filtered and concentrated under reduced pressure. The crude product was dissolved in MeOH (0.2 M) and refluxed overnight. The solvents were evaporated and the crude residue was purified using silica gel column chromatography, affording the β-ketoester.

**General procedure B**

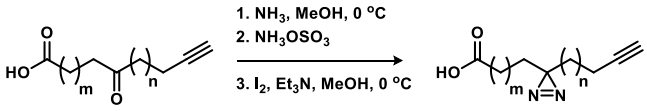


A round bottom flask was charged with ketoacid (1 eq) and dry MeOH (0.7 M) and cooled to 0 °C. Ammonia (7 M in MeOH, 21 eq) was added and the reaction was stirred for 4.5 h at 0 °C. Next, hydroxylamine-*O*-sulfonic acid (1.4 eq) was added and the mixture was stirred warming up to rt overnight. With a Pasteur pipette air was bubbled through the suspension for 1 h, followed by filtration of the formed $(NH_4)_2SO_4$ precipitate, washing with MeOH and concentration under reduced pressure. The crude residue was dissolved in dry MeOH (0.7 M), cooled to 0 °C and the flask was covered with aluminium foil. $Et_3N$ (1.5 eq) was added, followed by dropwise addition of a saturated solution of iodine in MeOH until the dark color persists. The reaction was quenched with 1 M aq. $Na_2S_2O_3$ and diluted with EtOAc. The organic layer was washed with 1 M aq. HCl (1x) and the aqueous layer was extracted again with EtOAc (1x). The combined organic layers were washed with brine (1x), dried ($Na_2SO_4$), filtered and concentrated under reduced pressure. The crude residue was purified using silica gel column chromatography, affording the diazirine product.

**General procedure C**

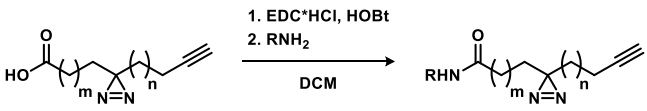


A round bottom flask covered with aluminium foil was charged with diazirine carboxylic acid (1 eq), EDC·HCl (1.5 eq), HOBt (1.5 eq) and dry DCM (0.2 M) and stirred for 1 h. Next, the amine (2 – 7 eq) was added and the reaction was stirred overnight. The mixture was concentrated under reduced pressure, dissolved in EtOAc and sequentially washed with 1 M aq. HCl (2x), sat. aq. $NaHCO_3$ (2x) and brine (1x). Each aqueous layer was back-extracted with EtOAc (1x) and the combined organic layers were dried ($MgSO_4$), filtered and concentrated under reduced pressure. The crude residue was purified using silica gel column chromatography, affording the amide product.

**General procedure D**

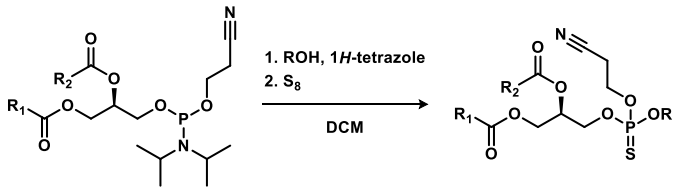


A round bottom flask was charged with phosphoramidite (1 eq), ethanolamide (1.1 eq), 1*H*-tetrazole (2 eq) and dry DCM (0.2 M) and stirred for 75 min. Sulfur ($S_8$, 20 eq) was added and the mixture was stirred overnight. The solvents were evaporated under reduced pressure and the crude residue was purified using silica gel column chromatography, affording the thiophosphotriester product.

*NAPE-based photoprobes **1-7***

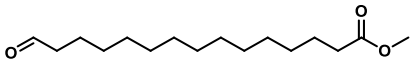

**Methyl 15-oxopentadecanoate (10).** *Esterification:* A round bottom flask was charged with 15-hydroxypentadecanoic acid **8** (1.0 g, 4.0 mmol, 1 eq) and MeOH (10 mL) and was cooled with a water bath. Acetylchloride (1.4 mL, 20 mmol, 5 eq) was added carefully and the reaction was stirred for 3.5 h. The solvents were evaporated and coevaporated with toluene (1x). The mixture was dissolved in DCM (40 mL) and washed with sat. aq. $NaHCO_3$ (1 x 40 mL), brine (1 x 40 mL), dried ($Na_2SO_4$), filtered and concentrated under reduced pressure, affording the methyl ester **9** (0.91 g, 3.3 mmol, 83%). *Oxidation:* A round bottom flask was charged with methyl ester **9** (0.91 g, 3.3 mmol, 83%) and DCM (16 mL). Pyridinium chlorochromate (1.2 g, 5.6 mmol, 1.7 eq) and Celite (1.2 g, 20 mmol, 6 eq) were added and the reaction was stirred for 2 h. The reaction was diluted with $Et_2O$ (50 mL) and the mixture was filtered over a plug of Celite and washed extensively with $Et_2O$. The solvents were evaporated under reduced pressure and the crude residue was purified by column chromatography (1% -> 20% EtOAc in pentane) affording the aldehyde **10** (0.66 g, 2.5 mmol, 74%), which was in accordance with reported NMR data.[50] $^1$H NMR (400 MHz, $CDCl_3$) δ 9.93 – 9.59 (m, 1H), 3.66 (s, 3H), 2.51 – 2.36 (m, 2H), 2.30 (t, *J* = 7.5 Hz, 2H), 1.71 – 1.54 (m, 4H), 1.37 – 1.20 (m, 18H). $^{13}$C NMR (101 MHz, $CDCl_3$) δ 202.80, 174.24, 51.38, 43.89, 34.06, 29.58, 29.55, 29.42, 29.35, 29.25, 29.15, 29.14, 24.94, 22.07.

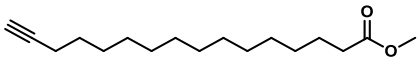

**Methyl hexadec-15-ynoate (11).** A round bottom flask was charged with the aldehyde **10** (0.66 g, 2.5 mmol, 1 eq) and MeOH (12 mL) and cooled to 0 °C. Ohira-Bestmann reagent (0.88 mL, 3.7 mmol, 1.5 eq) and $K_2CO_3$ (0.68 g, 4.9 mmol, 2 eq) were added and the mixture was stirred for 30 min at 0 °C and warmed to rt overnight. The reaction was quenched with sat. aq. $NH_4Cl$ (10 mL) and extracted with $Et_2O$ (4 x 50 mL). The combined organic layers were washed with brine (1 x 150 mL), dried ($MgSO_4$), filtered and concentrated under reduced pressure. The crude residue was purified by column chromatography (1% -> 3% EtOAc in pentane) affording the alkyne **11** (0.26 g, 0.98 mmol, 40%). $^1$H NMR (400 MHz, $CDCl_3$) δ 3.66 (s, 3H), 2.30 (t, *J* = 7.6 Hz, 2H), 2.17 (td, *J* = 7.1, 2.6 Hz, 2H), 1.94 (t, *J* = 2.7 Hz, 1H), 1.62 (p, *J* = 7.3 Hz, 2H), 1.57 – 1.46 (m, 2H), 1.44 – 1.35 (m, 2H), 1.35 – 1.15 (m, 16H). $^{13}$C NMR (101 MHz, $CDCl_3$) δ 174.22, 84.66, 68.11, 51.39, 34.10, 29.64, 29.62, 29.61, 29.54, 29.48, 29.30, 29.18, 29.15, 28.79, 28.53, 24.98, 18.41. HRMS [$C_{17}H_{30}O_2$ + H]$^+$: 267.2319 calculated, 267.2319 found.

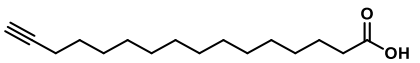

**Hexadec-15-ynoic acid (12).** A round bottom flask was charged with alkyne methyl ester **11** (0.26 g, 0.98 mmol, 1 eq), THF (3 mL) and 1.5 M NaOH (aq, 3 mL, 4.5 mmol, 4.5 eq). The reaction was stirred vigorously overnight after which 1 M HCl (30 mL). The aqueous layer was extracted with EtOAc (50 mL) and the organic layer was washed with brine (1 x 50 mL), dried ($Na_2SO_4$), filtered and concentrated under reduced pressure affording the carboxylic acid **12** (0.25 g, 0.98 mmol, quant), which was used for the next

step without further purification. $^{1}$H NMR (400 MHz, $CDCl_3$) δ 10.44 (br s, 1H), 2.34 (t, *J* = 7.5 Hz, 2H), 2.18 (td, *J* = 7.1, 2.6 Hz, 2H), 1.94 (t, *J* = 2.6 Hz, 1H), 1.63 (p, *J* = 7.4 Hz, 2H), 1.52 (p, *J* = 7.0 Hz, 2H), 1.45 – 1.36 (m, 2H), 1.35 – 1.23 (m, 16H). $^{13}$C NMR (101 MHz, $CDCl_3$) δ 180.20, 84.83, 68.15, 34.20, 29.69, 29.67, 29.66, 29.59, 29.52, 29.34, 29.20, 29.16, 28.85, 28.59, 24.78, 18.48. HRMS $[C_{16}H_{28}O_2 + H]^+$: 253.2162 calculated, 253.2164 found.

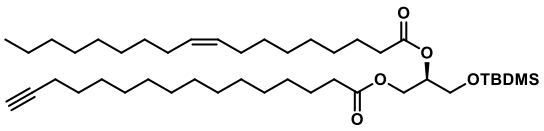


**(*R*)-1-((*tert*-Butyldimethylsilyl)oxy)-3-(hexadec-15-ynoyl-oxy)propan-2-yl oleate (13).**A 10 mL round bottom flask was charged with **12** (100 mg, 0.40 mmol, 1 eq) and (*S*,*S*)-(+)-*N*,*N*′-bis(3,5-di-*tert*-butylsalicylidene)-1,2-cyclohexane-diaminocobalt(II) (2.4 mg, 4 μmol, 1 mol%) in $Et_2O$ (1 mL) and stirred under an $O_2$ atmosphere (balloon). After 15 min the solvent was evaporated and DiPEA (70 μL, 0.40 mmol, 1 eq) and *tert*-butyldimethylsilyl (*R*)-(–)-glycidyl ether (87 μL, 0.40 mmol, 1 eq) were added. The reaction mixture was stirred overnight under an $O_2$ atmosphere, after which the solvents were concentrated under reduced pressure. The crude residue was purified by column chromatography (5 -> 25% EtOAc/pentane), affording the *sn*-1-monoacylglycerol (100 mg, 0.23 mmol, 57%). The product was dissolved in heptane (1 mL) and cooled to 0 °C under an argon atmosphere. Next, oleic acid (215 μL, 0.68 mmol, 3 eq), DMAP (3 mg, 0.03 mmol, 10 mol%) and DIC (43 μL, 0.28 mmol, 1.2 eq) were added. After 30 min the reaction was warmed to rt and stirred overnight. The solvents were concentrated under reduced pressure and the crude residue was purified by column chromatography (2.5% -> 5% EtOAc in pentane) affording the mixed diacylglycerol **13** (98 mg, 0.14 mmol, 60%). $^{1}$H NMR (400 MHz, $CDCl_3$) δ 5.43 – 5.26 (m, 2H), 5.12 – 5.03 (m, 1H), 4.34 (dd, *J* = 11.8, 3.7 Hz, 1H), 4.16 (dd, *J* = 11.8, 6.3 Hz, 1H), 3.78 – 3.64 (m, 2H), 2.30 (td, *J* = 7.6, 2.2 Hz, 4H), 2.18 (td, *J* = 7.1, 2.6 Hz, 2H), 2.01 (q, *J* = 6.4 Hz, 4H), 1.93 (t, *J* = 2.6 Hz, 1H), 1.66 – 1.57 (m, 4H), 1.57 – 1.47 (m, 2H), 1.41 – 1.36 (m, 2H), 1.36 – 1.21 (m, 36H), 0.92 – 0.85 (m, 12H), 0.05 (s, 6H). $^{13}$C NMR (101 MHz, $CDCl_3$) δ 173.56, 173.19, 130.11, 129.82, 84.87, 71.79, 68.16, 62.56, 61.57, 34.46, 34.28, 32.04, 29.89, 29.84, 29.73, 29.64, 29.60, 29.45, 29.42, 29.33, 29.25, 29.21, 28.89, 28.62, 27.34, 27.30, 25.88, 25.06, 25.04, 22.82, 18.52, 18.33, 14.25, -5.34, -5.38. HRMS $[C_{43}H_{80}O_5Si + H]^+$: 705.5848 calculated, 705.5852 found. $[\alpha]_D$ = +7.2 (c = 0.92 in $CHCl_3$).

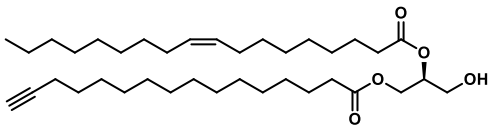


**(*S*)-1-(Hexadec-15-ynoyloxy)-3-hydroxypropan-2-yl oleate (14).** A round bottom flask was charged with protected diacylglycerol **13** (45 mg, 64 μmol, 1 eq) and a mixture of THF/$CH_3CN$ (1:1, 1 mL). $Et_3N{\cdot}3HF$ (125 μL, 0.76 mmol, 12 eq) was added and the reaction was stirred overnight. The mixture was cooled to 0 °C and quenched with sat. aq. $NaHCO_3$ (10 mL). The aqueous phase was extracted with DCM (3 x 20 mL) and the combined organic layers were washed with brine (1 x 50 mL), dried ($Na_2SO_4$), filtered and concentrated under reduced pressure. The crude residue was purified by column chromatography (10% -> 30% EtOAc in pentane) affording the diacylglyerol **14** (35 mg, 59 μmol, 93%). $^{1}$H NMR (400 MHz, $CDCl_3$) δ 5.42 – 5.27 (m, 2H), 5.08 (p, *J* = 5.0 Hz, 1H), 4.32 (dd, *J* = 11.9, 4.5 Hz, 1H), 4.23 (dd, *J* = 11.9, 5.7 Hz, 1H), 3.73 (d, *J* = 5.0 Hz, 2H), 2.40 – 2.28 (m, 4H), 2.18 (td, *J* = 7.1, 2.6 Hz, 2H), 2.01 (q, *J* = 6.2 Hz, 4H), 1.94 (t, *J* = 2.6 Hz, 1H), 1.68 – 1.57 (m, 4H), 1.57 – 1.47 (m, 2H), 1.42 – 1.20 (m, 39H), 0.88 (t, *J* = 6.8 Hz, 3H). $^{13}$C NMR (101 MHz, $CDCl_3$) δ 173.92, 173.54, 130.16, 129.82, 84.94, 72.25, 68.17, 62.15, 61.68, 34.42, 34.24, 32.04, 29.90, 29.84, 29.73, 29.66, 29.64, 29.60, 29.46, 29.40, 29.32, 29.25, 29.20, 28.90, 28.64, 27.36, 27.31, 25.06, 25.02, 22.82, 18.54, 14.25. HRMS $[C_{37}H_{66}O_5 + H]^+$: 591.4983 calculated, 591.4982 found. $[\alpha]_D$ = -2.3 (c = 0.7 in $CHCl_3$).

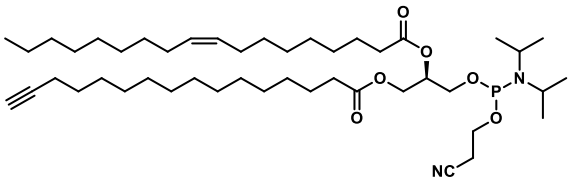

**(2*R*)-1-(((2-Cyanoethoxy)(diisopropylamino)phosphan-yl)oxy)-3-(hexadec-15-ynoyloxy)propan-2-yl oleate (15).** A round bottom flask was charged with **14** (32 mg, 54 μmol, 1 eq), DiPEA (38 μL, 0.22 mmol, 4 eq) and dry DCM (1 mL). 2-Cyanoethyl *N*,*N*-diisopropylchloro-phosphoramidite (24 μL, 0.11 mmol, 2 eq) was added. The reaction mixture was stirred for 30 min then quenched with sat. aq. $NaHCO_3$ in ice (20 mL). EtOAc (20 mL) was added and the organic layer was separated, washed with $H_2O$ (2 x 20 mL) and brine (1 x 20 mL), dried ($Na_2SO_4$), filtered and concentrated under reduced pressure. The crude residue was purified by column chromatography (pre-treat silica gel with 90:5:5 pentane/EtOAc/$Et_3N$, elute 90:5:5 pentane/EtOAc/$Et_3N$), affording the phosphoramidite **15** (42 mg, 53 μmol, 98%). $^1$H NMR (400 MHz, $CDCl_3$) δ 5.41 – 5.27 (m, 2H), 5.24 – 5.13 (m, 1H), 4.40 – 4.30 (m, 1H), 4.17 (td, *J* = 11.5, 6.3 Hz, 1H), 3.90 – 3.74 (m, 3H), 3.74 – 3.66 (m, 1H), 3.66 – 3.52 (m, 2H), 2.63 (t, *J* = 6.4 Hz, 2H), 2.38 – 2.25 (m, 4H), 2.18 (td, *J* = 7.1, 2.6 Hz, 2H), 2.08 – 1.96 (m, 4H), 1.93 (t, *J* = 2.6 Hz, 1H), 1.67 – 1.57 (m, 4H), 1.56 – 1.47 (m, 2H), 1.42 – 1.21 (m, 38H), 1.21 – 1.09 (m, 12H), 0.88 (t, *J* = 6.8 Hz, 3H). $^{13}$C NMR (101 MHz, $CDCl_3$) δ 173.49, 173.07, 130.13, 129.82, 117.64, 84.91, 70.84, 70.80, 70.76, 70.73, 68.16, 62.51, 62.50, 61.94, 61.78, 61.63, 58.73, 58.64, 58.54, 58.46, 43.37, 43.36, 43.25, 43.23, 34.43, 34.25, 32.03, 29.90, 29.85, 29.83, 29.74, 29.65, 29.64, 29.60, 29.45, 29.42, 29.34, 29.27, 29.24, 29.22, 28.89, 28.63, 27.35, 27.31, 25.04, 25.02, 24.75, 24.68, 22.81, 20.53, 20.46, 18.53, 14.24. $^{31}$P NMR (162 MHz, $CDCl_3$) δ 149.92, 149.77.

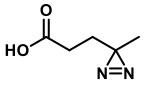

**3-(3-Methyl-3*H*-diazirin-3-yl)propanoic acid (17).** The title compound was prepared according to general procedure B using levulinic acid **16** (1.0 mL, 10 mmol, 1 eq), ammonia (7 M in MeOH, 10 mL, 70 mmol, 7 eq), hydroxylamine-*O*-sulfonic acid (1.3 g, 12 mmol, 1.15 eq) and $Et_3N$ (2.1 mL, 15 mmol, 1.5 eq), affording the product **17** (0.60 g, 4.7 mmol, 47%), which was in accordance with reported NMR data.[51] $^1$H NMR (400 MHz, $CDCl_3$) δ 10.87 (br s, 1H), 2.31 – 2.23 (m, 2H), 1.80 – 1.65 (m, 2H), 1.05 (s, 3H). $^{13}$C NMR (101 MHz, $CDCl_3$) δ 178.71, 29.31, 28.53, 25.07, 19.59.

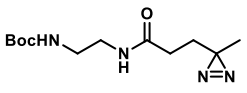

***tert*-Butyl (2-(3-(3-methyl-3*H*-diazirin-3-yl)propanamido)ethyl)carbamate (18).** A round bottom flask was charged with carboxylic acid **12** (81 mg, 0.63 mmol, 1 eq) and DCM (3 mL). EDC·HCl (182 mg, 0.95 mmol, 1.5 eq) and HOSu (109 mg, 0.95 mmol, 1.5 eq) were added and the mixture was stirred for 3 h. DiPEA (0.33 mL, 1.9 mmol, 3 eq) and *N*-Boc-ethylenediamine (0.11 mL, 0.69 mmol, 1.1 eq) were added and the reaction was stirred overnight. The mixture was diluted with EtOAc (50 mL) and washed with 0.1 M HCl (2 x 50 mL), sat. aq. $NaHCO_3$ (1 x 50 mL), brine (1 x 50 mL), dried ($Na_2SO_4$), filtered and concentrated under reduced pressure. The crude residue was purified by column chromatography (20% -> 80% EtOAc in pentane), affording the amide **18** (0.12 g, 0.45 mmol, 71%). $^1$H NMR (400 MHz, $CDCl_3$) δ 6.55 – 6.35 (m, 1H), 5.16 – 5.05 (m, 1H), 3.40 – 3.32 (m, 2H), 3.32 – 3.22 (m, 2H), 2.12 – 1.93 (m, 2H), 1.75 (t, *J* = 7.7 Hz, 2H), 1.44 (s, 9H), 1.03 (s, 3H). $^{13}$C NMR (101 MHz, $CDCl_3$) δ 172.15, 79.83, 40.94, 40.24, 30.73, 30.13, 25.56, 19.97. HRMS $[C_{12}H_{22}N_4O_3 + H]^+$: 271.1765 calculated, 271.1762 found.

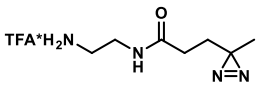

***N*-(2-Aminoethyl)-3-(3-methyl-3*H*-diazirin-3-yl)propanamide TFA salt (19).** A round bottom flask was charged with Boc-protected amine **18** (115 mg, 0.43 mmol, 1 eq) and a mixture of TFA/DCM (1:1, 4 mL). The reaction was stirred for 1 h after which the solvents were evaporated under reduced pressure. The residue was coevaporated with toluene (3x) affording the product as the TFA salt **19** (122 mg, 0.43 mmol, quant), which was used without further purification.

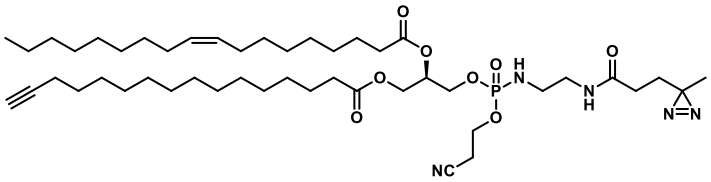

**(2*R*)-1-(((2-Cyanoethoxy)((2-(3-(3-methyl-3*H*-diazirin-3-yl)propanamido)-ethyl)-amino)-phosphoryl)-oxy)-3-(hexadec-15-ynoyloxy)propan-2-yl oleate (20).** *H-phosphonate formation:* A round bottom flask was charged with phosphoramidite **15** (24 mg, 30 μmol, 1 eq), 1*H*-tetrazole (4 mg, 56 μmol, 2 eq) and $CH_3CN$ (1 mL). The mixture was stirred for 10 min, after which $H_2O$ was added (100 μL) and then further stirred for 25 min. The reaction was diluted with DCM (20 mL) and washed with brine (1 x 20 mL), dried ($MgSO_4$), filtered and concentrated under reduced pressure, affording the *H*-phosphonate intermediate (22 mg, 31 μmol, quant). *Phosphoramidate synthesis:* A round bottom flask was charged with TFA salt **19** (20 mg, 70 μmol, 2.2 eq), $CCl_4$ (12 μL, 124 μmol, 4 eq), $Et_3N$ (43 μL, 0.31 mmol, 10 eq) and $CH_3CN$ (0.5 mL). The *H*-phosphonate (22 mg, 31 μmol, 1 eq) was taken up in DCM (1.2 mL) and added to the mixture via syringe. The reaction was stirred for 2.5 h after which the solvents were evaporated under reduced pressure. The crude residue was purified by column chromatography (2% -> 6% MeOH in DCM), affording the phosphoramidate **20** (15 mg, 17 μmol, 55%). $^1$H NMR (600 MHz, $CDCl_3$) δ 6.49 – 6.26 (m, 1H), 5.39 – 5.31 (m, 2H), 5.30 – 5.23 (m, 1H), 4.34 (ddd, *J* = 11.8, 7.6, 4.1 Hz, 1H), 4.28 – 3.97 (m, 5H), 3.59 – 3.46 (m, 1H), 3.42 – 3.28 (m, 2H), 3.18 – 3.03 (m, 2H), 2.77 (t, *J* = 6.0 Hz, 2H), 2.38 – 2.28 (m, 4H), 2.18 (td, *J* = 7.2, 2.6 Hz, 2H), 2.06 – 1.97 (m, 6H), 1.94 (t, *J* = 2.6 Hz, 1H), 1.80 (t, *J* = 7.6 Hz, 2H), 1.66 – 1.57 (m, 4H), 1.55 – 1.49 (m, 2H), 1.42 – 1.37 (m, 2H), 1.37 – 1.20 (m, 36H), 1.04 (s, 3H), 0.88 (t, *J* = 7.0 Hz, 3H). $^{13}$C NMR (151 MHz, $CDCl_3$) δ 173.59, 173.57, 173.26, 173.19, 172.26, 172.25, 130.17, 129.79, 117.04, 84.95, 69.65, 69.62, 69.60, 69.58, 68.18, 64.85, 64.82, 64.73, 64.70, 61.89, 61.81, 61.19, 61.15, 41.20, 41.17, 41.02, 40.99, 40.96, 34.31, 34.15, 32.04, 30.62, 29.90, 29.87, 29.86, 29.76, 29.74, 29.74, 29.66, 29.64, 29.62, 29.46, 29.42, 29.35, 29.28, 29.26, 29.25, 29.20, 28.90, 28.62, 27.36, 27.31, 25.78, 24.98, 24.97, 22.82, 20.10, 19.97, 19.93, 18.53, 14.27. $^{31}$P NMR (162 MHz, $CDCl_3$) δ 9.55, 9.43. HRMS $[C_{47}H_{82}N_5O_8P + H]^+$: 876.5974 calculated, 876.5982 found.

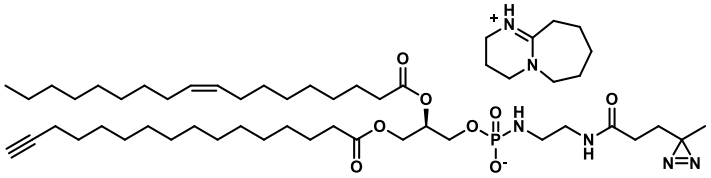

**(*R*)-3-(hexadec-15-ynoyloxy)-2-(oleoyloxy)-propyl (2-(3-(3-methyl-3*H*-diazirin-3-yl)-propanamido)-ethyl)-phosphoramidate DBU-H$^+$ salt (1).** A round bottom flask was charged with protected phosphoramidate **20** (13 mg, 15 μmol, 1 eq), 1,8-diazabicyclo[5.4.0]undec-7-ene (2.5 μL, 17 μmol, 1.1 eq) and DCM (0.5 mL). The mixture was stirred for 2 h after which the solvents were evaporated under reduced pressure and the residue was coevaporated with toluene (2x). The crude residue was purified by column chromatography (10% -> 20% MeOH in DCM), affording the phosphoramidate as the DBU salt **1** (6 mg, 6.2 μmol, 41%). $^1$H NMR (600 MHz, $CDCl_3$ + MeOD) δ 5.35 – 5.27 (m, 2H), 5.22 – 5.16 (m, 1H), 4.39 (dd, *J* = 12.0, 3.0 Hz, 1H), 4.16 (dd, *J* = 12.0, 6.9 Hz, 1H), 3.94 – 3.83 (m, 2H), 3.61 – 3.56 (m, 2H), 3.54 (t, *J* = 5.9 Hz, 2H), 3.35 (t, *J* = 5.8 Hz, 2H), 3.21 (t, *J* = 5.8 Hz, 2H), 2.98 – 2.90 (m, 2H), 2.70 – 2.63 (m, 2H), 2.36 – 2.25 (m, 4H), 2.14 (td, *J* = 7.1, 2.6 Hz, 2H), 2.08 – 2.03 (m, 4H), 2.03 – 1.95 (m, 5H), 1.83 – 1.78 (m, 2H), 1.78 – 1.70 (m, 4H), 1.70 – 1.64 (m, 2H), 1.63 – 1.53 (m, 4H), 1.48 (p, *J* = 7.1 Hz, 2H), 1.41 – 1.35 (m, 2H), 1.34 – 1.19 (m, 36H), 1.00 (s, 3H), 0.86 (t, *J* = 7.0 Hz, 3H). $^{13}$C NMR (151 MHz, $CDCl_3$ + MeOD) δ 174.56, 174.18, 173.80, 166.81, 130.47, 130.20, 84.99, 78.37, 78.16, 77.94, 71.37, 71.31, 68.66, 63.36, 63.23, 63.20, 55.08, 42.27, 41.13, 38.78, 34.77, 34.61, 33.28, 32.46, 30.94, 30.88, 30.28, 30.16, 30.14, 30.06, 30.05, 29.86, 29.82, 29.80, 29.69, 29.68, 29.65, 29.39, 29.27, 29.08, 27.70, 27.69, 27.02, 25.88, 25.47, 25.43, 24.39, 23.19, 19.88, 19.79, 18.75, 14.33. $^{31}$P NMR (162 MHz, $CDCl_3$ + MeOD) δ 6.86. HRMS $[C_{44}H_{79}N_4O_8P + H]^+$: 823.5708 calculated, 823.5702 found.

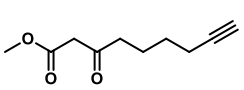

**Methyl 3-oxonon-8-ynoate (24).** The title compound was prepared according to general procedure A using 6-heptynoic acid **21** (1.1 mL, 8.9 mmol, 1 eq), Meldrum's acid (1.6 g, 11 mmol, 1.1 eq), DMAP (1.5 g, 12 mmol, 1.3 eq) and DIC (1.8 mL, 12 mmol, 1.3 eq). Column chromatography (10% -> 20% EtOAc in pentane) afforded the product **24** (1.2 g, 6.7 mmol, 74%). $^{1}$H NMR (400 MHz, $CDCl_3$) δ 3.74 (s, 3H), 3.46 (s, 2H), 2.58 (t, *J* = 7.3 Hz, 2H), 2.21 (td, *J* = 7.0, 2.7 Hz, 2H), 1.97 (t, *J* = 2.6 Hz, 1H), 1.77 – 1.67 (m, 2H), 1.60 – 1.50 (m, 2H). $^{13}$C NMR (101 MHz, $CDCl_3$) δ 202.35, 167.65, 83.91, 68.74, 52.36, 49.00, 42.37, 27.63, 22.46, 18.20. HRMS $[C_{10}H_{14}O_3 + H]^+$: 183.1016 calculated, 183.1016 found.

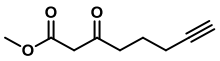

**Methyl 3-oxooct-7-ynoate (25).** The title compound was prepared according to general procedure A using 5-hexynoic acid **22** (2.2 mL, 20 mmol, 1 eq), Meldrum's acid (3.2 g, 22 mmol, 1.1 eq), DMAP (2.9 g, 24 mmol, 1.2 eq) and DIC (3.7 mL, 24 mmol, 1.2 eq). Column chromatography (5% -> 10% EtOAc in pentane) afforded the product **25** (1.8 g, 10.4 mmol, 52%). $^{1}$H NMR (300 MHz, $CDCl_3$) δ 3.74 (s, 3H), 3.50 (s, 2H), 2.71 (t, *J* = 7.2 Hz, 2H), 2.24 (td, *J* = 6.9, 2.7 Hz, 2H), 2.02 (t, *J* = 2.7 Hz, 1H), 1.81 (p, *J* = 7.0 Hz, 2H). $^{13}$C NMR (75 MHz, $CDCl_3$) δ 202.00, 167.43, 83.20, 69.21, 52.17, 48.91, 41.19, 21.82, 17.37. HRMS $[C_9H_{12}O_3 + H]^+$: 169.0859 calculated, 169.0859 found.

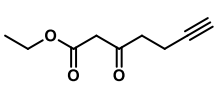

**Ethyl 3-oxohept-6-ynoate (26).** The title compound was prepared according to general procedure A using 4-pentynoic acid **23** (2.0 g, 20 mmol, 1 eq), Meldrum's acid (3.2 g, 22 mmol, 1.1 eq), DMAP (2.9 g, 24 mmol, 1.2 eq) and DIC (3.7 mL, 24 mmol, 1.2 eq). Column chromatography (5% -> 10% EtOAc in pentane) afforded the product **26** (2.0 g, 11.5 mmol, 58%). $^{1}$H NMR (300 MHz, $CDCl_3$) δ 4.27 – 4.12 (m, 2H), 3.48 (s, 2H), 2.89 – 2.73 (m, 2H), 2.48 (td, *J* = 7.2, 2.6 Hz, 2H), 2.01 – 1.94 (m, 1H), 1.34 – 1.23 (m, 3H). $^{13}$C NMR (75 MHz, $CDCl_3$) δ 200.64, 166.94, 82.57, 69.04, 61.51, 49.21, 41.61, 14.11, 12.82. HRMS $[C_9H_{12}O_3 + H]^+$: 169.0859 calculated, 169.0859 found.

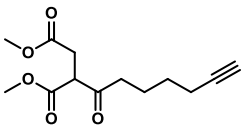

**Dimethyl 2-(hept-6-ynoyl)succinate (27).** A round bottom flask was charged with β-ketoester **24** (1.2 g, 6.7 mmol, 1 eq) and NaOMe (0.47 g, 8.6 mmol, 1.3 eq) and dry MeOH (30 mL) and stirred for 30 min. Next, methyl bromoacetate (0.82 mL, 8.7 mmol, 1.3 eq) was added and the reaction mixture was stirred at reflux temperature for 3.5 h. The solvents were removed under reduced pressure and the crude residue was dissolved in EtOAc. The organic layer was washed with water (1 x 120 mL) and brine (1 x 120 mL), dried ($MgSO_4$), filtered and concentrated under reduced pressure. The crude residue was purified by column chromatography (10% -> 20% EtOAc in pentane) affording the product **27** (1.1 g, 4.4 mmol, 66%) and recovered starting material (0.23 g, 2.0 mmol, 19%). $^{1}$H NMR (400 MHz, $CDCl_3$) δ 3.99 (dd, *J* = 8.4, 6.1 Hz, 1H), 3.75 (s, 3H), 3.68 (s, 3H), 3.00 (dd, *J* = 17.6, 8.5 Hz, 1H), 2.84 (dd, *J* = 17.5, 6.1 Hz, 1H), 2.80 – 2.60 (m, 2H), 2.20 (td, *J* = 7.0, 2.6 Hz, 2H), 1.96 (t, *J* = 2.6 Hz, 1H), 1.78 – 1.68 (m, 2H), 1.59 – 1.48 (m, 2H). $^{13}$C NMR (101 MHz, $CDCl_3$) δ 203.53, 171.81, 168.88, 84.00, 68.66, 53.74, 52.78, 52.07, 42.19, 32.20, 27.64, 22.46, 18.23. HRMS $[C_{13}H_{18}O_5 + H]^+$: 255.1227 calculated, 255.1226 found.

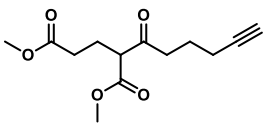

**Dimethyl 2-(hex-5-ynoyl)pentanedioate (28).** A round bottom flask was charged with β-ketoester **25** (1.7 g, 10 mmol, 1 eq), $K_2CO_3$ (1.4 g, 10 mmol, 1 eq), methyl acrylate (0.93 mL, 10 mmol, 1 eq) and DCM (50 mL). The mixture was stirred for 20 h at rt, followed by addition of methyl acrylate (0.47 mL, 5.1 mmol, 0.5 eq) and stirring for 4 h at rt, then for 16 h at reflux. DMF (20 mL) was added and the reaction was refluxed for 4 h, after which starting material was consumed as judged by TLC analysis. $H_2O$ was added (50 mL) and the mixture was extracted with $Et_2O$ (3 x 50 mL). The combined organic layers were washed with water (2 x 100 mL), brine (1 x 100 mL), dried ($MgSO_4$), filtered and concentrated under reduced pressure. The crude residue was purified by column chromatography (5% -> 30% EtOAc in pentane) affording the product **28** (1.4 g, 5.5 mmol, 53%). $^{1}$H NMR (300 MHz, $CDCl_3$) δ 3.74 (s, 3H), 3.70 – 3.58 (m, 4H), 2.90 – 2.58 (m, 2H), 2.41 – 2.30 (m, 2H), 2.22 (td, *J* = 6.9, 2.7 Hz, 2H), 2.18 – 2.08 (m, 2H), 2.05 (t, *J* = 2.6 Hz, 1H), 1.79 (p, *J* = 7.0 Hz, 2H).

$^{13}$C NMR (75 MHz, $CDCl_3$) δ 203.70, 172.65, 169.29, 82.99, 69.04, 56.94, 52.08, 51.24, 40.15, 30.81, 22.64, 21.67, 17.09. HRMS $[C_{13}H_{18}O_5 + H]^+$: 255.1227 calculated, 255.1224 found.

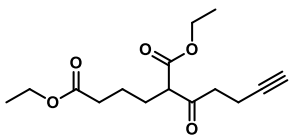

**Diethyl 2-(pent-4-ynoyl)hexanedioate (29).** A round bottom flask was charged with β-ketoester **26** (1.9 g, 11.4 mmol, 1 eq), NaOEt (0.86 g, 12.6 mmol, 1.1 eq), NaI (0.16 g, 1.1 mmol, 0.1 eq) and dry EtOH (11 mL) and stirred for 30 min. Next, a solution of ethyl 4-bromobutanoate (2.3 mL, 16.1 mmol, 1.4 eq) in EtOH (16 mL) was added dropwise and the reaction mixture was stirred at reflux overnight. Additional NaOEt (2.7 M in EtOH, 2.6 mL, 6.9 mmol, 0.6 eq) was added and the reaction was stirred for 0.5 h. The solvents were removed under reduced pressure and the crude residue was dissolved in 0.5 M HCl (aq, 75 mL) and extracted with $Et_2O$ (3 x 60 mL). The combined organic layers were washed with $H_2O$ (2 x 180 mL), dried ($MgSO_4$), filtered and concentrated under reduced pressure. The crude residue was purified by column chromatography (5% -> 20% EtOAc in pentane) affording the product **29** (1.2 g, 4.3 mmol, 38%) and recovered starting material (0.38 g, 2.3 mmol, 20%). $^1$H NMR (300 MHz, $CDCl_3$) δ 4.26 – 4.07 (m, 4H), 3.48 (t, *J* = 7.3 Hz, 1H), 2.94 – 2.66 (m, 2H), 2.46 (td, *J* = 7.3, 2.6 Hz, 2H), 2.33 (t, *J* = 7.3 Hz, 2H), 1.97 (t, *J* = 2.7 Hz, 1H), 1.95 – 1.83 (m, 2H), 1.68 – 1.54 (m, 2H), 1.27 (q, *J* = 7.2 Hz, 6H). $^{13}$C NMR (75 MHz, $CDCl_3$) δ 202.73, 172.94, 169.23, 82.65, 68.94, 61.54, 60.38, 58.61, 40.59, 33.84, 27.36, 22.66, 14.23, 14.11, 12.86. HRMS $[C_{15}H_{22}O_5 + H]^+$: 283.1540 calculated, 283.1535 found.

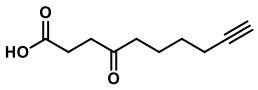

**4-Oxodec-9-ynoic acid (30).** A round bottom flask was charged with ketodiester **27** (1.7 g, 6.9 mmol, 1 eq), THF (40 mL) and 1 M NaOH (aq, 40 mL, 40 mmol, 5.8 eq) and the reaction was stirred vigorously overnight. The mixture was cooled to 0 °C and 3 M HCl (aq, 60 mL) was added carefully. The reaction was stirred at rt for 2 h and at 55°C for 1 h. The mixture was extracted with EtOAc (3 x 100 mL) and the combined organic layers were washed with brine (1 x 200 mL), dried ($MgSO_4$), filtered and concentrated under reduced pressure. The crude residue was purified by column chromatography (40% -> 60% EtOAc in pentane + 0.5% AcOH) affording the ketoacid **30** (1.3 g, 6.9 mmol, quant). $^1$H NMR (400 MHz, $CDCl_3$ + MeOD) δ 2.74 (t, *J* = 6.4 Hz, 2H), 2.58 (t, *J* = 6.4 Hz, 2H), 2.51 (t, *J* = 7.3 Hz, 2H), 2.20 (td, *J* = 6.8, 2.2 Hz, 2H), 2.05 – 1.96 (m, 1H), 1.71 (p, *J* = 7.3 Hz, 2H), 1.53 (p, *J* = 7.1 Hz, 2H). $^{13}$C NMR (101 MHz, $CDCl_3$ + MeOD) δ 209.70, 175.20, 83.76, 68.47, 41.85, 36.83, 27.59, 27.52, 22.54, 17.91. HRMS $[C_{10}H_{14}O_3 + H]^+$: 183.1016 calculated, 183.1016 found.

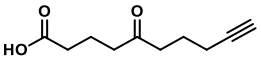

**5-Oxodec-9-ynoic acid (31).** A round bottom flask was charged with ketodiester **28** (1.4 g, 5.4 mmol, 1 eq), THF (32 mL) and 1 M NaOH (aq, 32 mL, 32 mmol, 5.8 eq) and the reaction was stirred vigorously for 2 h. The mixture was cooled to 0 °C and 3 M HCl (aq, 47 mL) was added carefully, followed by stirring at 55 °C overnight. The mixture was extracted with EtOAc (3 x 80 mL) and the combined organic layers were washed with brine (1 x 160 mL), dried ($MgSO_4$), filtered and concentrated under reduced pressure. The crude residue was purified by column chromatography (40% -> 60% EtOAc in pentane + 0.5% AcOH) affording the ketoacid **31** (0.83 g, 4.6 mmol, 84%). $^1$H NMR (300 MHz, $CDCl_3$) δ 11.36 (br s, 1H), 2.57 (q, *J* = 7.5 Hz, 4H), 2.40 (t, *J* = 6.9 Hz, 2H), 2.22 (t, *J* = 6.6 Hz, 2H), 2.08 – 1.99 (m, 1H), 1.95 – 1.81 (m, 2H), 1.81 – 1.69 (m, 2H). $^{13}$C NMR (75 MHz, $CDCl_3$) δ 209.75, 178.61, 83.23, 69.03, 41.09, 40.74, 32.60, 21.89, 18.22, 17.33. HRMS $[C_{10}H_{14}O_3 + H]^+$: 183.1016 calculated, 183.1015 found.

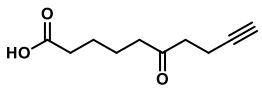

**6-Oxodec-9-ynoic acid (32).** A round bottom flask was charged with ketodiester **29** (1.2 g, 4.2 mmol, 1 eq), THF (25 mL) and 1 M NaOH (aq, 25 mL, 25 mmol, 5.8 eq) and the reaction was stirred vigorously for 2 h. The mixture was cooled to 0 °C and 3 M HCl (aq, 47 mL) was added carefully, followed by stirring at 55 °C overnight. The mixture was extracted with EtOAc (3 x 60 mL) and the combined organic layers were washed with brine (1 x 120 mL), dried ($MgSO_4$), filtered and concentrated under reduced pressure. The crude residue was purified by column chromatography (40% -> 60% EtOAc in pentane + 0.5% AcOH) affording the ketoacid **32** (0.63 g, 3.4 mmol,

82%). $^{1}$H NMR (300 MHz, $CDCl_3$) δ 11.47 (s, 1H), 2.68 (t, *J* = 7.1 Hz, 2H), 2.55 – 2.30 (m, 6H), 2.02 – 1.94 (m, 1H), 1.75 – 1.55 (m, 4H). $^{13}$C NMR (75 MHz, $CDCl_3$) δ 208.39, 179.53, 82.97, 68.76, 42.12, 41.10, 33.64, 23.93, 22.80, 12.82. HRMS $[C_{10}H_{14}O_3 + H]^+$: 183.1016 calculated, 183.1015 found.

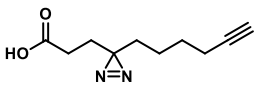

**3-(3-(Hex-5-yn-1-yl)-3*H*-diazirin-3-yl)propanoic acid (33).** The title compound was prepared according to general procedure B using ketoacid **30** (1.3 g, 6.9 mmol, 1 eq), ammonia (7 M in MeOH, 13 mL, 91 mmol, 21 eq), hydroxylamine-*O*-sulfonic acid (1.1 g, 9.8 mmol, 1.4 eq) and $Et_3N$ (1.5 mL, 10.5 mmol, 1.5 eq). Column chromatography (10% -> 40% EtOAc in pentane + 0.5% AcOH) afforded the product **33** (0.69 g, 3.5 mmol, 51%). $^{1}$H NMR (400 MHz, $CDCl_3$) δ 10.89 (br s, 1H), 2.21 – 2.12 (m, 4H), 1.96 (t, *J* = 2.6 Hz, 1H), 1.75 (t, *J* = 7.7 Hz, 2H), 1.53 – 1.40 (m, 4H), 1.28 – 1.18 (m, 2H). $^{13}$C NMR (101 MHz, $CDCl_3$) δ 178.85, 83.94, 68.78, 32.28, 28.42, 27.96, 27.93, 27.85, 22.96, 18.22. HRMS $[C_{10}H_{14}N_2O_2 + H]^+$: 195.1128 calculated, 195.1128 found.

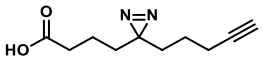

**4-(3-(Pent-4-yn-1-yl)-3H-diazirin-3-yl)butanoic acid (34).** The title compound was prepared according to general procedure B using ketoacid **31** (0.83 g, 4.6 mmol, 1 eq), ammonia (7 M in MeOH, 13.7 mL, 96 mmol, 21 eq), hydroxylamine-*O*-sulfonic acid (0.73 g, 6.4 mmol, 1.4 eq) and $Et_3N$ (0.95 mL, 6.8 mmol, 1.5 eq). Column chromatography (10% -> 40% EtOAc in pentane + 0.5% AcOH) afforded the product **34** (0.49 g, 2.5 mmol, 55%). $^{1}$H NMR (300 MHz, $CDCl_3$) δ 11.50 (br s, 1H), 2.38 – 2.27 (m, 2H), 2.16 (td, *J* = 6.9, 2.6 Hz, 2H), 1.97 (t, *J* = 2.6 Hz, 1H), 1.57 – 1.49 (m, 2H), 1.49 – 1.40 (m, 4H), 1.39 – 1.29 (m, 2H). $^{13}$C NMR (75 MHz, $CDCl_3$) δ 179.64, 83.31, 69.11, 33.26, 32.13, 31.53, 28.00, 22.67, 18.96, 17.89. HRMS $[C_{10}H_{14}N_2O_2 + H]^+$: 195.1128 calculated, 195.1128 found.

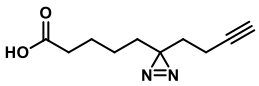

**5-(3-(But-3-yn-1-yl)-3*H*-diazirin-3-yl)pentanoic acid (35).** The title compound was prepared according to general procedure B using ketoacid **32** (0.62 g, 3.4 mmol, 1 eq), ammonia (7 M in MeOH, 10.2 mL, 71 mmol, 21 eq), hydroxylamine-*O*-sulfonic acid (0.54 g, 4.8 mmol, 1.4 eq) and $Et_3N$ (0.71 mL, 5.1 mmol, 1.5 eq). Column chromatography (10% -> 40% EtOAc in pentane + 0.5% AcOH) afforded the product **35** (0.25 g, 1.3 mmol, 38%) and recovered starting material (0.16 g, 0.89 mmol, 26%). $^{1}$H NMR (300 MHz, $CDCl_3$) δ 10.91 (br s, 1H), 2.33 (t, *J* = 7.4 Hz, 2H), 2.09 – 1.94 (m, 3H), 1.61 (ddd, *J* = 15.5, 8.6, 4.9 Hz, 4H), 1.53 – 1.41 (m, 2H), 1.30 – 1.05 (m, 2H). $^{13}$C NMR (75 MHz, $CDCl_3$) δ 179.61, 69.26, 33.81, 32.50, 32.39, 28.17, 24.22, 23.44, 13.44. HRMS $[C_{10}H_{14}N_2O_2 + H]^+$: 195.1128 calculated, 195.1127 found.

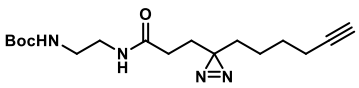

***tert*-Butyl (2-(3-(3-(hex-5-yn-1-yl)-3*H*-diazirin-3-yl)propanamido)ethyl)-carbamate (36).** The title compound was prepared according to general procedure C using carboxylic acid **33** (80 mg, 0.41 mmol, 1 eq), EDC·HCl (118 mg, 0.62 mmol, 1.5 eq), HOBt (84 mg, 0.62 mmol, 1.5 eq) and *N*-Boc-ethylenediamine (129 μL, 0.82 mmol, 2 eq). Column chromatography (50% -> 100% EtOAc in pentane) afforded the product Boc protected amide **36** (134 mg, 0.40 mmol, 97%). $^{1}$H NMR (400 MHz, $CDCl_3$) δ 6.71 – 6.47 (m, 1H), 5.30 – 5.17 (m, 1H), 3.33 (q, *J* = 5.3 Hz, 2H), 3.30 – 3.18 (m, 2H), 2.15 (td, *J* = 7.0, 2.4 Hz, 2H), 1.98 – 1.88 (m, 3H), 1.78 (t, *J* = 7.6 Hz, 2H), 1.51 – 1.40 (m, 13H), 1.28 – 1.19 (m, 2H). $^{13}$C NMR (101 MHz, $CDCl_3$) δ 172.12, 157.01, 83.94, 79.67, 68.73, 40.71, 40.18, 32.42, 30.43, 28.58, 28.41, 28.33, 27.84, 22.94, 18.20. HRMS $[C_{17}H_{28}N_4O_3 + H]^+$: 337.2234 calculated, 337.2230 found.

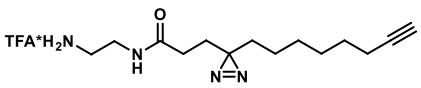

***N*-(2-Aminoethyl)-3-(3-(oct-7-yn-1-yl)-3*H*-diazirin-3-yl)propanamide TFA salt (37).** A round bottom flask was charged with Boc-protected amine **36** (133 mg, 0.40 mmol, 1 eq) and a mixture of TFA/DCM (1:1, 3 mL). The reaction was stirred for 1.5 h after which the solvents were evaporated under reduced pressure. The residue was coevaporated with toluene (3x) affording the product as the TFA salt **37** (140 mg, 0.40 mmol, quant), which was used without further purification.

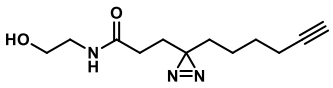

**3-(3-(Hex-5-yn-1-yl)-3*H*-diazirin-3-yl)-*N*-(2-hydroxyethyl)propanamide (38).** The title compound was prepared according to general procedure C using carboxylic acid **33** (224 mg, 1.2 mmol, 1 eq), EDC·HCl (332 mg, 1.7 mmol, 1.5 eq), HOBt (234 mg, 1.7 mmol, 1.5 eq) and 2-aminoethanol (349 μL, 5.8 mmol, 5 eq). Column chromatography (0% -> 4% MeOH in EtOAc) afforded the amide product **38** (215 mg, 0.91 mmol, 78%). $^{1}$H NMR (400 MHz, $CDCl_3$) δ 6.63 (s, 1H), 3.70 (t, *J* = 5.1 Hz, 2H), 3.60 (s, 1H), 3.38 (q, *J* = 5.2 Hz, 2H), 2.16 (td, *J* = 7.0, 2.6 Hz, 2H), 2.03 – 1.90 (m, 3H), 1.80 (t, *J* = 7.7 Hz, 2H), 1.53 – 1.37 (m, 4H), 1.28 – 1.15 (m, 2H). $^{13}$C NMR (101 MHz, $CDCl_3$) δ 172.70, 114.72, 83.97, 68.77, 61.64, 42.35, 32.36, 30.39, 28.54, 28.40, 27.78, 22.91, 18.16. HRMS $[C_{12}H_{19}N_3O_2 + H]^+$: 238.1550 calculated, 238.1552 found.

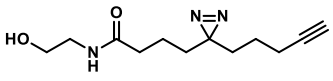

***N*-(2-Hydroxyethyl)-4-(3-(pent-4-yn-1-yl)-3*H*-diazirin-3-yl)butanamide (39).** The title compound was prepared according to general procedure C using carboxylic acid **34** (148 mg, 0.76 mmol, 1 eq), EDC·HCl (219 mg, 1.1 mmol, 1.5 eq), HOBt (154 mg, 1.1 mmol, 1.5 eq) and 2-aminoethanol (320 μL, 5.3 mmol, 7 eq). Column chromatography (0% -> 4% MeOH in EtOAc) afforded the amide product **39** (137 mg, 0.58 mmol, 76%). $^{1}$H NMR (400 MHz, $CDCl_3$) δ 6.83 – 6.68 (m, 1H), 3.96 (br s, 1H), 3.67 (t, *J* = 5.1 Hz, 2H), 3.37 (q, *J* = 5.3 Hz, 2H), 2.21 – 2.12 (m, 4H), 2.00 (t, *J* = 2.6 Hz, 1H), 1.55 – 1.48 (m, 2H), 1.48 – 1.39 (m, 4H), 1.37 – 1.27 (m, 2H). $^{13}$C NMR (101 MHz, $CDCl_3$) δ 173.55, 83.31, 69.13, 61.55, 42.22, 35.45, 32.12, 31.45, 28.13, 22.61, 19.97, 17.82. HRMS $[C_{12}H_{19}N_3O_2 + H]^+$: 238.1550 calculated, 238.1552 found.

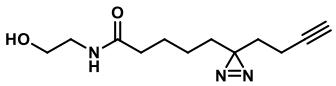

**5-(3-(But-3-yn-1-yl)-3*H*-diazirin-3-yl)-*N*-(2-hydroxyethyl)pentanamide (40).** The title compound was prepared according to general procedure C using carboxylic acid **35** (100 mg, 0.51 mmol, 1 eq), EDC·HCl (148 mg, 0.77 mmol, 1.5 eq), HOBt (104 mg, 0.77 mmol, 1.5 eq) and 2-aminoethanol (220 μL, 3.6 mmol, 7 eq). Column chromatography (0% -> 4% MeOH in EtOAc) afforded the amide product **40** (84 mg, 0.35 mmol, 69%). $^{1}$H NMR (400 MHz, $CDCl_3$) δ 6.55 – 6.47 (m, 1H), 3.73 – 3.66 (m, 2H), 3.58 (br s, 1H), 3.39 (q, *J* = 5.3 Hz, 2H), 2.17 (t, *J* = 7.5 Hz, 2H), 2.04 – 1.96 (m, 3H), 1.66 – 1.53 (m, 4H), 1.51 – 1.44 (m, 2H), 1.17 – 1.05 (m, 2H). $^{13}$C NMR (101 MHz, $CDCl_3$) δ 174.04, 82.84, 69.27, 61.91, 42.36, 36.20, 32.33, 32.27, 28.18, 25.13, 23.47, 13.33. HRMS $[C_{12}H_{19}N_3O_2 + H]^+$: 238.1550 calculated, 238.1552 found.

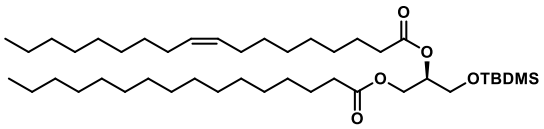

**(*R*)-1-((*tert*-Butyldimethylsilyl)oxy)-3-(palmitoyloxy)-propan-2-yl oleate (42).** A 10 mL round bottom flask was charged with palmitic acid (1.0 g, 4.0 mmol, 1 eq) and (*S*,*S*)-(+)-*N*,*N*′-bis(3,5-di-*tert*-butylsalicylidene)-1,2-cyclohexane-diaminocobalt(II) (24 mg, 0.04 mmol, 1 mol%) in $Et_2O$ (2 mL) and stirred under an $O_2$ atmosphere (balloon). After 75 min the solvent was evaporated and DiPEA (0.70 mL, 4.0 mmol, 1 eq) and *tert*-butyldimethylsilyl (*R*)-(–)-glycidyl ether **41** (0.87 mL, 4.0 mmol, 1 eq) were added. The reaction mixture was stirred overnight under an $O_2$ atmosphere, after which the solvents were concentrated under reduced pressure. The mixture was dissolved in heptane (8 mL) and cooled to 0 °C under an argon atmosphere. Next, oleic acid (1.5 mL, 4.7 mmol, 1.2 eq), DMAP (49 mg, 0.40 mmol, 10 mol%) and DIC (0.74 mL, 4.8 mmol, 1.2 eq) were added. After 30 min the reaction was warmed to rt and stirred overnight. The solvents were concentrated under reduced pressure and the crude residue was purified by column chromatography (0.5% -> 3% EtOAc in pentane) affording the diacylglycerol **42** (1.9 g, 2.6 mmol, 64%). $^{1}$H NMR (400 MHz, $CDCl_3$) δ 5.36 – 5.24 (m, 2H), 5.08 – 4.98 (m, 1H), 4.31 (dd, *J* = 11.8, 3.7 Hz, 1H), 4.12 (dd, *J* = 11.8, 6.3 Hz, 1H), 3.71 – 3.65 (m, 2H), 2.26 (td, *J* = 7.5, 2.6 Hz, 4H), 1.97 (q, *J* = 6.4 Hz, 4H), 1.63 – 1.53 (m, 4H), 1.24 (d, *J* = 17.6 Hz, 44H), 0.88 – 0.81 (m, 15H), 0.02 (s, 6H). $^{13}$C NMR (101 MHz, $CDCl_3$) δ 173.30, 172.95, 129.99, 129.71, 71.75, 62.45, 61.54, 34.36, 34.19, 32.02, 32.00, 29.84, 29.79, 29.75, 29.72, 29.62, 29.57, 29.46, 29.41, 29.38, 29.27, 29.21, 29.18, 29.15, 27.28, 27.23, 25.80, 24.99, 22.76,

18.23, 14.16, -5.45, -5.49. HRMS $[C_{43}H_{84}O_5Si + H]^+$: 709.6161 calculated, 709.6163 found. $[\alpha]_D$ = +7.7 (c = 3.0 in $CHCl_3$).

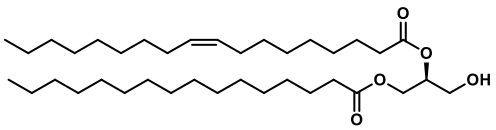

**(*S*)-1-((*tert*-Butyldimethylsilyl)oxy)-3-(palmitoyloxy)propan-2-yl oleate (43).** A round bottom flask was charged with protected diacylglycerol **42** (1.9 g, 2.6 mmol, 1 eq) and a mixture of THF/$CH_3CN$ (1:1, 20 mL). $Et_3N{\cdot}3HF$ (4.2 mL, 26 mmol, 10 eq) was added and the reaction was stirred overnight. The mixture was cooled to 0 °C and quenched with sat. aq. $NaHCO_3$ (120 mL). The aqueous phase was extracted with DCM (3 x 100 mL) and the combined organic layers were washed with brine (1 x 150 mL), dried ($Na_2SO_4$), filtered and concentrated under reduced pressure. The crude residue was purified by column chromatography (10% -> 30% EtOAc in pentane) affording the diacylglycerol **43** (1.5 g, 2.6 mmol, 99%). $^1$H NMR (400 MHz, $CDCl_3$) δ 5.42 – 5.25 (m, 2H), 5.09 (p, *J* = 5.1 Hz, 1H), 4.33 (dd, *J* = 11.9, 4.3 Hz, 1H), 4.22 (dd, *J* = 11.9, 5.9 Hz, 1H), 3.72 (d, *J* = 5.1 Hz, 2H), 2.60 (br s, 1H), 2.39 – 2.25 (m, 4H), 2.01 (q, *J* = 6.5 Hz, 4H), 1.72 – 1.53 (m, 4H), 1.39 – 1.19 (m, 44H), 0.88 (t, *J* = 6.8 Hz, 6H). $^{13}$C NMR (101 MHz, $CDCl_3$) δ 173.83, 173.48, 130.05, 129.73, 72.16, 62.22, 61.43, 34.36, 34.34, 34.17, 32.01, 31.99, 29.84, 29.79, 29.75, 29.71, 29.61, 29.57, 29.45, 29.41, 29.36, 29.27, 29.20, 29.18, 29.15, 27.29, 27.24, 25.01, 24.99, 24.96, 22.77, 14.18. HRMS $[C_{37}H_{70}O_5 + H]^+$: 595.5296 calculated, 595.5297 found. $[\alpha]_D$ = -1.7 (c = 1.2 in $CHCl_3$)

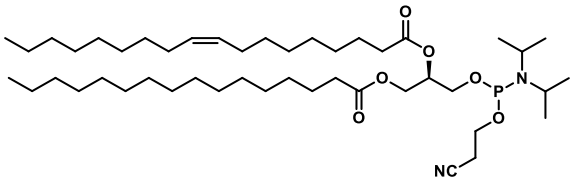

**(2*R*)-1-(((2-Cyanoethoxy)(diisopropylamino)-phosphan-yl)oxy)-3-(palmitoyloxy)propan-2-yl oleate (44).** A round bottom flask was charged with **43** (163 mg, 0.27 mmol, 1 eq), DiPEA (191 μL, 1.1 mmol, 4 eq) and dry DCM (3 mL). 2-Cyanoethyl *N*,*N*-diisopropylchlorophosphoramidite (90 μL, 0.41 mmol, 1.5 eq) was added. The reaction mixture was stirred for 45 min then quenched with sat. aq. $NaHCO_3$ in ice (30 mL). EtOAc (30 mL) was added and the organic layer was separated, washed with $H_2O$ (1 x 30 mL) and brine (1 x 30 mL), dried ($Na_2SO_4$), filtered and concentrated under reduced pressure. Column chromatography (pre-treat silica gel with 90:5:5 pentane/EtOAc/$Et_3N$, elute 93:5:2 pentane/EtOAc/$Et_3N$) afforded the phosphoramidite **44** (200 mg, 0.25 mmol, 260 mg, 93%). $^1$H NMR (400 MHz, $CDCl_3$) δ 5.41 – 5.27 (m, 2H), 5.26 – 5.12 (m, 1H), 4.42 – 4.27 (m, 1H), 4.17 (td, *J* = 11.6, 6.3 Hz, 1H), 3.92 – 3.74 (m, 3H), 3.74 – 3.65 (m, 1H), 3.65 – 3.52 (m, 2H), 2.63 (t, *J* = 6.4 Hz, 2H), 2.38 – 2.26 (m, 4H), 2.10 – 1.91 (m, 4H), 1.67 – 1.56 (m, 4H), 1.38 – 1.22 (m, 44H), 1.20 – 1.16 (m, 12H), 0.88 (t, *J* = 6.8 Hz, 6H). $^{13}$C NMR (101 MHz, $CDCl_3$) δ 173.44, 173.03, 130.08, 129.78, 117.61, 70.80, 70.76, 70.72, 70.69, 62.47, 62.45, 61.89, 61.74, 61.58, 58.70, 58.61, 58.51, 58.42, 43.32, 43.31, 43.20, 43.19, 34.42, 34.40, 34.22, 32.03, 32.01, 29.87, 29.81, 29.77, 29.74, 29.63, 29.59, 29.47, 29.43, 29.40, 29.31, 29.24, 29.19, 27.32, 27.28, 25.00, 24.72, 24.65, 22.80, 20.49, 20.43, 14.22. $^{31}$P NMR (162 MHz, $CDCl_3$) δ 149.49, 149.35.

**(2*R*)-1-(((2-Cyanoethoxy)((2-(3-(3-(hex-5-yn-1-yl)-3*H*-diazirin-3-yl)propanamido)ethyl)amino)phosphoryl)-oxy)-3-(palmitoyloxy)propan-2-yl oleate (45).**

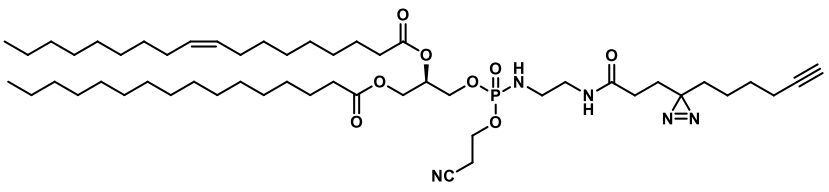

*H-phosphonate formation:* A round bottom flask was charged with phosphoramidite **44** (86 mg, 0.11 mmol, 1 eq), 1*H*-tetrazole (16 mg, 0.22 mmol, 2 eq) and $CH_3CN$ (2 mL). The mixture was stirred for 10 min, after which $H_2O$ was added (200 μL) and then further stirred for 30 min. The reaction was diluted with DCM (25

mL) and washed with brine (1 x 25 mL), dried ($MgSO_4$), filtered and concentrated under reduced pressure, affording the *H*-phosphonate intermediate (76 mg, 0.11 mmol, quant). *Phosphoramidate synthesis:* A round bottom flask was charged with TFA salt **37** (57 mg, 0.16 mmol, 1.5 eq) and $CH_3CN$ (0.5 mL) and cooled to 0 $^oC$. $CCl_4$ (64 μL, 0.66 mmol, 5 eq) and $Et_3N$ (153 μL, 1.1 mmol, 10 eq) were added and the *H*-phosphonate (76 mg, 0.11 mmol, 1 eq) was taken up in DCM (1 mL) and added to the mixture via syringe. After 5 min the reaction mixture was warmed to rt and stirred for 1.5 h. The solvents were evaporated under reduced pressure and coevaporated with toluene (1x). The crude residue was purified by column chromatography (2.5% -> 7.5% MeOH in DCM), affording the phosphoramidate **45** (81 mg, 86 μmol, 80%). $^1H$ NMR (400 MHz, $CDCl_3$) δ 6.65 – 6.48 (m, 1H), 5.40 – 5.31 (m, 2H), 5.29 – 5.23 (m, 1H), 4.35 (dd, *J* = 12.0, 3.9 Hz, 1H), 4.23 – 4.08 (m, 5H), 3.88 – 3.75 (m, 1H), 3.41 – 3.27 (m, 2H), 3.15 – 2.98 (m, 2H), 2.78 (t, *J* = 6.0 Hz, 2H), 2.33 (q, *J* = 7.9 Hz, 4H), 2.15 (td, *J* = 7.0, 2.6 Hz, 2H), 2.05 – 1.98 (m, 4H), 1.95 (t, *J* = 2.7 Hz, 1H), 1.94 – 1.87 (m, 2H), 1.86 – 1.78 (m, 2H), 1.66 – 1.58 (m, 4H), 1.52 – 1.44 (m, 2H), 1.44 – 1.38 (m, 2H), 1.37 – 1.20 (m, 46H), 0.88 (t, *J* = 6.7 Hz, 6H). $^{13}C$ NMR (101 MHz, $CDCl_3$) δ 173.49, 173.47, 173.08, 172.11, 130.10, 129.73, 116.99, 69.64, 69.61, 69.57, 69.54, 68.74, 64.74, 64.69, 64.65, 64.60, 61.89, 61.83, 61.15, 61.10, 41.14, 40.88, 34.25, 34.10, 32.58, 32.00, 30.34, 29.84, 29.78, 29.74, 29.60, 29.59, 29.44, 29.39, 29.30, 29.22, 29.19, 29.15, 28.57, 28.34, 27.90, 27.30, 27.26, 24.93, 23.01, 22.76, 19.91, 19.84, 18.25, 14.20. $^{31}P$ NMR (162 MHz, $CDCl_3$) δ 9.47, 9.38. HRMS $[C_{52}H_{92}N_5O_8P + H]^+$: 946.6756 calculated, 946.6759 found.

**(*R*)-2-(Oleoyloxy)-3-(palmitoyloxy)propyl(2-(3-(3-(hex-5-yn-1-yl)-3*H*-diazirin-3-yl)propanamido)ethyl) phosphoramidate triethylammonium salt (2).**

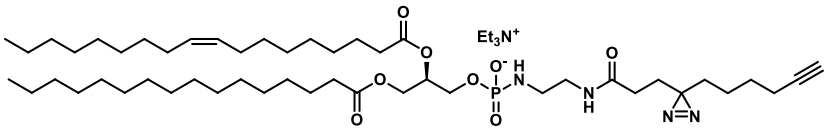


A round bottom flask was charged with protected phosphoramidate **45** (40 mg, 42 μmol, 1 eq), 1,8-diazabicyclo[5.4.0]undec-7-ene (8.6 μL, 57 μmol, 1.3 eq) and DCM (1 mL). The mixture was stirred for 2 h after which the solvents were evaporated under reduced pressure and the residue was coevaporated with toluene (2x). The crude residue was purified by column chromatography (pre-treat the silica gel with 85:5:10 DCM/MeOH/$Et_3N$, elute with 5% -> 10% MeOH in DCM), affording the phosphoramidate as the triethylammonium salt with $Et_3N{\cdot}HCl$ contamination. The product was taken up in 10% MeOH in $CHCl_3$, washed with MilliQ (3x) and concentrated under reduced pressure to give the phosphoramidate triethylammonium salt **2** (10 mg, 10 μmol, 24%). $^1H$ NMR (500 MHz, $CDCl_3$ + MeOD) δ 5.36 – 5.25 (m, *J* = 5.5 Hz, 2H), 5.21 – 5.13 (m, 1H), 4.34 (dd, *J* = 12.0, 3.0 Hz, 2H), 4.11 (dd, *J* = 12.0, 7.1 Hz, 2H), 3.90 – 3.77 (m, *J* = 5.9 Hz, 2H), 3.20 (t, *J* = 6.2 Hz, 2H), 3.12 (q, *J* = 7.3 Hz, 6H), 2.87 (dt, *J* = 12.0, 6.1 Hz, 2H), 2.31 – 2.24 (m, 4H), 2.11 (td, *J* = 7.0, 2.6 Hz, 2H), 2.02 – 1.93 (m, 6H), 1.74 – 1.68 (m, 2H), 1.60 – 1.54 (m, 4H), 1.47 – 1.41 (m, 2H), 1.41 – 1.36 (m, 2H), 1.33 (t, *J* = 7.3 Hz, 9H), 1.24 (d, *J* = 24.7 Hz, 44H), 0.84 (t, *J* = 6.9 Hz, 6H). $^{13}C$ NMR (126 MHz, $CDCl_3$ + MeOD) δ 174.34, 173.96, 173.53, 130.32, 129.93, 84.09, 70.93, 70.86, 68.96, 63.05, 46.72, 41.58, 40.85, 34.52, 34.38, 32.46, 32.23, 30.54, 30.05, 30.00, 29.98, 29.96, 29.85, 29.82, 29.67, 29.62, 29.57, 29.46, 29.45, 29.40, 29.04, 28.58, 28.13, 27.49, 27.46, 25.17, 23.19, 22.97, 18.37, 14.25, 8.82. $^{31}P$ NMR (202 MHz, $CDCl_3$ + MeOD) δ 5.37. HRMS $[C_{49}H_{89}N_4O_8P + H]^+$: 893.6491 calculated, 893.6491 found.

**(2*R*)-1-(((2-Cyanoethoxy)((2-(3-(3-(hex-5-yn-1-yl)-3*H*-diazirin-3-yl)propanamido)ethyl)amino) phosphorothioyl)oxy)-3-(palmitoyloxy)propan-2-yl oleate (46).**

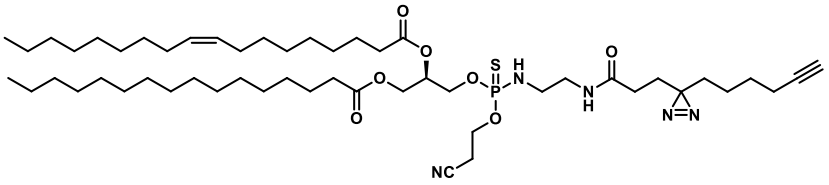

*H-thiophosphonate formation:* A round bottom flask was charged with phosphoramidite **44** (72 mg, 91 μmol, 1 eq), 1*H*-tetrazole (13 mg, 0.18 mmol, 2 eq) and dry $CH_3CN$ (2 mL). The mixture was stirred for 10 min, after which $H_2S$ (0.8 M in THF, 1.1 mL, 0.91 mmol, 10 eq) was added and then further stirred for 1 h. Argon was bubbled through the reaction mixture and the flow of $H_2S$ was quenched by bleach. The reaction was quenched with sat. aq. $NaHCO_3$ (25 mL) and the aqueous layer was extracted with DCM (2 x 25 mL). The combined organic layers were washed with brine (1 x 25 mL), dried ($MgSO_4$), filtered and concentrated under reduced pressure, affording the product as a mixture of *H*-thiophosphonate and *H*-phosphonate (1 : 0.4, 67 mg in total). *Thiophosphoramidate synthesis:* A round bottom flask was charged with TFA salt **37** (53 mg, 0.15 mmol, 1.6 eq) and $CH_3CN$ (0.5 mL) and cooled to 0 °C. $CCl_4$ (45 μL, 0.47 mmol, 5 eq) and $Et_3N$ (129 μL, 0.93 mmol, 10 eq) were added and the *H*-thiophosphonate/H-phosphonate mixture (67 mg) was taken up in DCM (1 mL) and added to the mixture via syringe. After 5 min the reaction mixture was warmed to rt and stirred for 2 h. The solvents were evaporated under reduced pressure and coevaporated with toluene (1x). The crude residue was purified by column chromatography (2% -> 4% MeOH in DCM), affording the thiophosphoramidate **46** (20 mg, 21 μmol, 31%). $^1$H NMR (500 MHz, $CDCl_3$) δ 6.13 (t, *J* = 5.3 Hz, 1H), 5.40 – 5.30 (m, 2H), 5.31 – 5.23 (m, 1H), 4.38 – 4.29 (m, 1H), 4.25 – 4.14 (m, 4H), 4.14 – 4.05 (m, 1H), 3.71 – 3.61 (m, 1H), 3.41 – 3.27 (m, 2H), 3.23 – 3.11 (m, 2H), 2.77 (t, *J* = 6.0 Hz, 2H), 2.34 (q, *J* = 7.8 Hz, 4H), 2.16 (td, *J* = 7.0, 2.6 Hz, 2H), 2.07 – 1.97 (m, 4H), 1.97 – 1.90 (m, 3H), 1.83 (t, *J* = 7.1 Hz, 2H), 1.67 – 1.56 (m, 4H), 1.51 – 1.44 (m, 2H), 1.44 – 1.38 (m, 2H), 1.38 – 1.19 (m, 46H), 0.88 (t, *J* = 6.9 Hz, 6H). $^{13}$C NMR (126 MHz, $CDCl_3$) δ 173.63, 173.61, 173.28, 173.20, 172.24, 130.17, 129.80, 117.19, 84.09, 77.41, 77.16, 76.91, 69.63, 69.56, 68.77, 65.20, 65.16, 65.00, 64.96, 61.97, 61.89, 61.50, 61.47, 41.67, 40.85, 40.81, 34.35, 34.20, 32.64, 32.06, 30.44, 29.90, 29.84, 29.80, 29.66, 29.64, 29.50, 29.46, 29.35, 29.28, 29.20, 28.61, 28.39, 28.37, 27.96, 27.36, 27.31, 24.99, 23.07, 22.83, 19.73, 19.67, 18.32, 14.27. $^{31}$P NMR (202 MHz, $CDCl_3$) δ 74.40, 74.16. HRMS $[C_{52}H_{92}N_5O_7PS + H]^+$ : 962.6528 calculated, 962.6531 found.

***O*-((*R*)-2-(Oleoyloxy)-3-(palmitoyloxy)propyl)(2-(3-(3-(hex-5-yn-1-yl)-3*H*-diazirin-3-yl)propanamido)ethyl) phosphoramidothioate *tert*-butylammonium salt (3).**

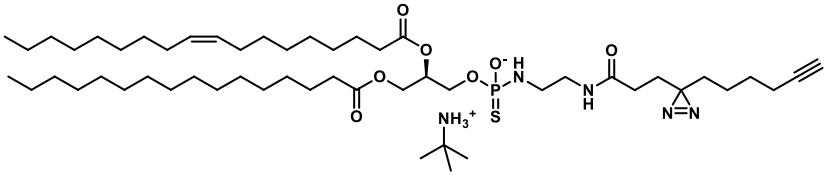

A round bottom flask was charged with protected thiophosphoramidate **46** (19 mg, 20 μmol, 1 eq) was dissolved in dry DCM (0.75 mL). *tert*-Butylamine (0.75 mL, 7.1 mmol, 350 eq) was added and the reaction mixture was stirred for 5 hours, after which the solvents were evaporated, affording the thiophosphoramidate as the pure *tert*-butylammonium salt **3** (20 mg, 20 μmol, quant). $^1$H NMR (500 MHz, $CDCl_3$ + MeOD) δ 5.41 – 5.30 (m, 2H), 5.30 – 5.19 (m, 1H), 4.23 – 4.15 (m, 1H), 4.06 – 3.98 (m, 1H), 3.98 – 3.88 (m, 1H), 3.31 – 3.17 (m, 2H), 3.10 – 2.97 (m, 2H), 2.38 – 2.28 (m, 4H), 2.16 (td, *J* = 7.0, 2.6 Hz, 2H), 2.07 – 1.95 (m, 7H), 1.80 – 1.71 (m, 2H), 1.67 – 1.55 (m, 4H), 1.53 – 1.45 (m, 2H), 1.45 – 1.40 (m, 2H), 1.39 (s, 9H), 1.29 (d, *J* = 24.0 Hz, 44H), 1.24 – 1.18 (m, 2H), 0.88 (q, *J* = 6.1, 5.5 Hz, 6H). *1H from (sn-1 $CH_2$) underneath*

*$H_2O$ solvent*. $^{13}$C NMR (126 MHz, $CDCl_3$ + MeOD) δ 174.41, 174.01, 173.95, 173.20, 130.27, 129.97, 100.35, 84.13, 71.01, 70.94, 70.89, 70.82, 68.92, 63.53, 63.50, 63.45, 63.18, 51.83, 49.51, 49.34, 49.17, 49.00, 48.83, 48.66, 48.49, 41.78, 41.77, 41.75, 41.74, 40.81, 40.79, 34.58, 34.42, 32.45, 32.22, 32.20, 30.53, 30.04, 30.03, 29.98, 29.96, 29.94, 29.80, 29.65, 29.61, 29.59, 29.54, 29.44, 29.42, 29.38, 29.09, 28.59, 28.14, 27.66, 27.48, 27.45, 25.19, 25.16, 23.19, 22.96, 18.36, 14.24. $^{31}$P NMR (202 MHz, $CDCl_3$ + MeOD) δ 60.66, 60.55. HRMS $[C_{49}H_{89}N_4O_7PS + H]^+$: 909.6262 calculated, 909.6276 found.

**(2*R*)-1-(((2-Cyanoethoxy)(2-(3-(3-(hex-5-yn-1-yl)-3*H*-diazirin-3-yl)propanamido)ethoxy)phosphorothioyl)oxy)-3-(palmitoyloxy)propan-2-yl oleate (47).**

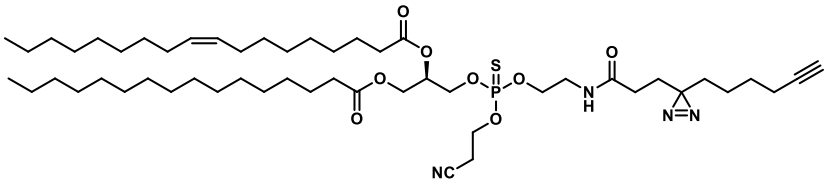

The title compound was prepared according to General Procedure D using phosphoramidite **44** (66 mg, 83 μmol, 1 eq), ethanolamide **38** (22 mg, 91 μmol, 1.1 eq), 1*H*-tetrazole (12 mg, 166 μmol, 2 eq) and sulfur ($S_8$, 50 mg, 1.6 mmol, 19 eq). Column chromatography (0% -> 2% MeOH in DCM) afforded the thiophosphotriester product **47** (47 mg, 49 μmol, 59%). $^1$H NMR (400 MHz, $CDCl_3$) δ 6.44 – 6.16 (m, 1H), 5.40 – 5.30 (m, 2H), 5.29 – 5.22 (m, 1H), 4.36 – 4.09 (m, 8H), 3.57 – 3.49 (m, 2H), 2.77 (td, *J* = 6.1, 3.0 Hz, 2H), 2.34 (q, *J* = 7.5 Hz, 4H), 2.15 (td, *J* = 7.0, 2.6 Hz, 2H), 2.09 – 1.89 (m, 7H), 1.83 – 1.77 (m, 2H), 1.67 – 1.56 (m, 4H), 1.52 – 1.44 (m, 2H), 1.44 – 1.38 (m, 2H), 1.37 – 1.23 (m, 46H), 0.88 (t, *J* = 6.8 Hz, 6H). $^{13}$C NMR (101 MHz, $CDCl_3$) δ 173.56, 173.51, 173.24, 173.10, 171.97, 130.15, 129.78, 116.76, 116.72, 84.07, 69.46, 69.38, 69.30, 68.72, 67.95, 67.90, 67.86, 67.80, 66.49, 66.44, 66.39, 66.35, 62.72, 62.68, 62.64, 61.83, 61.75, 53.56, 39.69, 39.67, 39.62, 39.60, 34.31, 34.29, 34.16, 32.54, 32.04, 30.30, 29.88, 29.81, 29.64, 29.61, 29.48, 29.43, 29.41, 29.32, 29.25, 29.17, 28.54, 28.43, 27.96, 27.34, 27.29, 24.96, 23.06, 22.80, 19.70, 19.63, 18.30, 14.24. $^{31}$P NMR (162 MHz, $CDCl_3$) δ 69.26. HRMS $[C_{52}H_{91}N_4O_8PS + H]^+$: 963.6368 calculated, 963.6375 found.

***O*-(2-(3-(3-(Hex-5-yn-1-yl)-3*H*-diazirin-3-yl)propanamido)ethyl)-*O*-((*R*)-2-(oleoyloxy)-3-(palmitoyloxy)propyl) phosphorothioate (4).**

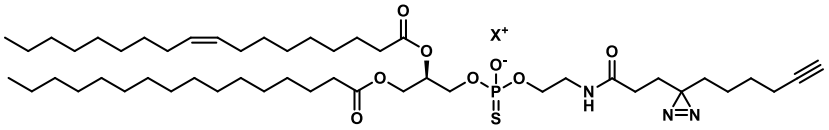

A round bottom flask was charged with thiophosphotriester **48** (47 mg, 49 μmol, 1 eq) was dissolved in dry DCM (0.5 mL). *tert*-Butylamine (0.5 mL, 4.8 mmol, 100 eq) was added and the reaction mixture was stirred for 3 hours, after which the solvents were evaporated. The crude residue was purified by column chromatography with high-purity grade silica gel (1% -> 10% MeOH in DCM), affording the thiophosphodiester **4** as a salt with undefined cation (36 mg, 40 μmol, 81%, based on the free anion). $^1$H NMR (500 MHz, $CDCl_3$ + MeOD) δ 5.36 – 5.25 (m, 2H), 5.24 – 5.17 (m, 1H), 4.37 – 4.31 (m, 1H), 4.17 – 4.10 (m, 1H), 4.08 – 3.89 (m, 4H), 3.45 – 3.34 (m, 2H), 2.29 (q, *J* = 7.2 Hz, 4H), 2.12 (td, *J* = 7.0, 2.7 Hz, 2H), 2.03 – 1.92 (m, 7H), 1.74 – 1.68 (m, 2H), 1.63 – 1.53 (m, 4H), 1.48 – 1.41 (m, 2H), 1.41 – 1.36 (m, 2H), 1.33 – 1.17 (m, 46H), 0.92 – 0.77 (m, 6H). $^{13}$C NMR (126 MHz, $CDCl_3$ + MeOD) δ 174.39, 173.98, 173.95, 173.49, 130.33, 130.00, 84.12, 70.68, 70.65, 70.61, 70.58, 69.04, 64.74, 64.70, 64.66, 64.54, 64.51, 64.45, 64.40, 62.97, 40.42, 40.37, 34.59, 34.46, 32.50, 32.28, 32.26, 30.55, 30.10, 30.05, 30.03, 30.01, 29.87, 29.72, 29.68, 29.65, 29.61, 29.51, 29.50, 29.45, 29.12, 28.58, 28.20, 27.54, 27.51, 25.25, 25.23, 23.26, 23.02, 18.42, 14.28. $^{31}$P NMR (162 MHz, $CDCl_3$ + MeOD) δ 54.95. HRMS $[C_{49}H_{87}N_3O_8PS + H]^+$: 910.6103 calculated, 910.6106 found.

**(2*R*)-1-(((2-(5-(3-(But-3-yn-1-yl)-3*H*-diazirin-3-yl)pentanamido)ethoxy)(2-cyanoethoxy)phosphoro-thioyl)oxy)-3-(palmitoyloxy)propan-2-yl oleate (48).**

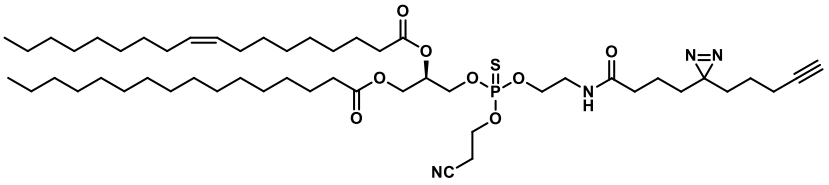

The title compound was prepared according to General Procedure D using phosphoramidite **44** (69 mg, 86 μmol, 1 eq), ethanolamide **39** (21 mg, 88 μmol, 1 eq), 1*H*-tetrazole (0.45 M in $CH_3CN$, 0.39 mL, 0.18 mmol, 2 eq) and sulfur ($S_8$, 50 mg, 1.6 mmol, 18 eq). Column chromatography (0% -> 2% MeOH in DCM) afforded the thiophosphotriester product **48** (35 mg, 37 μmol, 42%). $^1$H NMR (500 MHz, $CDCl_3$) δ 6.38 – 6.20 (m, 1H), 5.39 – 5.30 (m, 2H), 5.30 – 5.23 (m, 1H), 4.38 – 4.09 (m, 8H), 3.59 – 3.48 (m, 2H), 2.82 – 2.73 (m, 2H), 2.38 – 2.30 (m, 4H), 2.21 – 2.13 (m, 4H), 2.06 – 1.97 (m, 4H), 1.95 (t, *J* = 2.6 Hz, 1H), 1.67 – 1.56 (m, 4H), 1.54 – 1.48 (m, 2H), 1.44 – 1.37 (m, 2H), 1.36 – 1.22 (m, 48H), 0.88 (t, *J* = 6.9 Hz, 6H). $^{13}$C NMR (126 MHz, $CDCl_3$) δ 173.52, 173.47, 173.18, 173.06, 172.68, 172.66, 130.14, 129.76, 116.75, 116.72, 83.47, 69.41, 69.35, 69.28, 69.11, 68.01, 67.97, 67.91, 67.87, 66.46, 66.44, 66.40, 66.36, 62.71, 62.68, 62.64, 61.80, 61.73, 39.57, 39.55, 39.51, 39.49, 35.54, 35.53, 34.29, 34.27, 34.15, 32.45, 32.42, 32.04, 32.02, 31.61, 29.87, 29.82, 29.78, 29.75, 29.64, 29.61, 29.48, 29.44, 29.41, 29.33, 29.24, 29.17, 28.27, 27.33, 27.29, 24.95, 22.81, 20.07, 20.05, 19.70, 19.64, 18.03, 14.25. $^{31}$P NMR (162 MHz, $CDCl_3$) δ 69.31. HRMS $[C_{52}H_{91}N_4O_8PS + H]^+$: 963.6368 calculated, 963.6383 found.

***O*-((*R*)-2-(Oleoyloxy)-3-(palmitoyloxy)propyl)-*O*-(2-(4-(3-(pent-4-yn-1-yl)-3*H*-diazirin-3-yl)butan-amido)ethyl) phosphorothioate triethylammonium salt (6).**

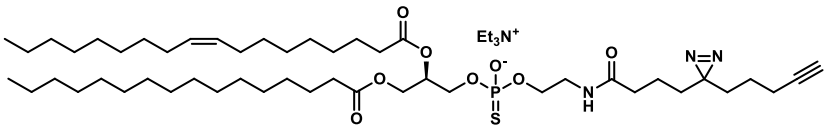

A round bottom flask was charged with thiophosphotriester **48** (35 mg, 37 μmol, 1 eq) and dry DCM (1.5 mL). *tert*-Butylamine (0.5 mL, 4.8 mmol, 130 eq) was added and the reaction mixture was stirred for 3.5 hours, after which the solvent was evaporated. Column chromatography with high-purity grade silica gel (5% MeOH in DCM + 0.5% $Et_3N$) gave the desired product on $^1$H-NMR and $^{13}$C-NMR but not on $^{31}$P-NMR, suggesting that metals cations were chelating the thiophosphate. The product was dissolved in a 1:1 mixture of MilliQ and 10% MeOH in $CHCl_3$ (2 mL) and EDTA-$Na_2$ (56 mg, 0.17 mmol, 4.6 eq) was added. After stirring for 30 min a clear peak was observed again by $^{31}$P-NMR. The mixture was washed with MilliQ (2 x 20 mL) and the combined aqueous layers were back-extracted with 10% MeOH in $CHCl_3$. The combined organic layers were concentrated under reduced pressure and purified by column chromatography with high-purity grade silica gel (5% MeOH in DCM + 0.5% $Et_3N$), affording the thiophosphodiester product as the triethylammonium salt **6** (7.6 μmol, 7.7 mg, 21%). $^1$H NMR (500 MHz, $CDCl_3$ + MeOD) δ 5.35 – 5.26 (m, 2H), 5.26 – 5.19 (m, 1H), 4.37 (dd, *J* = 12.0, 3.3 Hz, 1H), 4.18 – 4.12 (m, 1H), 4.10 – 3.91 (m, 4H), 3.43 – 3.37 (m, 2H), 3.14 (q, *J* = 7.3 Hz, 6H), 2.29 (q, *J* = 7.3 Hz, 4H), 2.17 – 2.09 (m, 4H), 2.04 – 1.90 (m, 5H), 1.62 – 1.54 (m, 4H), 1.52 – 1.45 (m, 2H), 1.45 – 1.35 (m, 4H), 1.34 – 1.20 (m, 55H), 0.88 – 0.81 (m, 6H). $^{13}$C NMR (126 MHz, $CDCl_3$ + MeOD) δ 174.40, 174.19, 173.96, 130.37, 130.09, 83.63, 70.80, 70.72, 69.41, 65.01, 64.96, 64.96, 64.92, 64.62, 64.58, 64.50, 63.05, 46.73, 40.53, 40.48, 35.78, 34.66, 34.53, 32.81, 32.34, 32.32, 31.96, 30.16, 30.10, 30.06, 29.92, 29.76, 29.72, 29.70, 29.65, 29.55, 29.50, 28.49, 27.59, 27.57, 25.30, 23.16, 23.06, 20.50, 18.19, 14.28, 8.88. $^{31}$P NMR (202 MHz, MeOD) δ 59.73, 59.70. HRMS $[C_{49}H_{87}N_3O_8PS + H]^+$: 910.6103 calculated, 910.6105 found.

**(2*R*)-1-(((2-Cyanoethoxy)(2-(4-(3-(pent-4-yn-1-yl)-3*H*-diazirin-3-yl)butanamido)ethoxy)phosphoro-thioyl)oxy)-3-(palmitoyloxy)propan-2-yl oleate (49).**

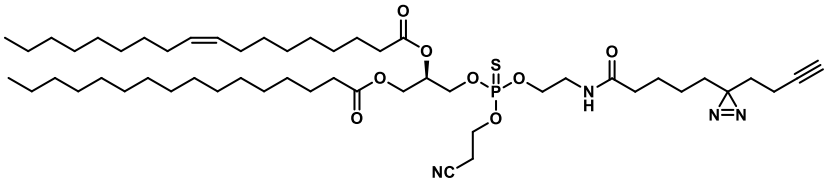

The title compound was prepared according to General Procedure D using phosphoramidite **44** (72 mg, 91 μmol, 1.05 eq), ethanolamide **40** (21 mg, 86 μmol, 1 eq), 1*H*-tetrazole (0.45 M in $CH_3CN$, 0.39 mL, 0.18 mmol, 2 eq) and sulfur ($S_8$, 50 mg, 1.6 mmol, 17 eq). Column chromatography (0% -> 2% MeOH in DCM) afforded the thiophosphotriester product **49** (29 mg, 30 μmol, 35%). $^1$H NMR (500 MHz, $CDCl_3$) δ 6.35 – 6.18 (m, 1H), 5.40 – 5.31 (m, 2H), 5.30 – 5.23 (m, 1H), 4.37 – 4.11 (m, 8H), 3.60 – 3.48 (m, 2H), 2.77 (td, *J* = 6.0, 3.4 Hz, 2H), 2.38 – 2.30 (m, 4H), 2.18 (td, *J* = 7.5, 4.1 Hz, 2H), 2.06 – 1.95 (m, 7H), 1.67 – 1.55 (m, 8H), 1.49 – 1.43 (m, 2H), 1.36 – 1.21 (m, 44H), 1.16 – 1.08 (m, 2H), 0.88 (t, *J* = 6.9 Hz, 6H). $^{13}$C NMR (126 MHz, $CDCl_3$) δ 173.51, 173.47, 173.17, 173.12, 173.10, 173.06, 130.15, 129.77, 116.76, 116.73, 82.91, 69.41, 69.35, 69.29, 69.21, 68.06, 68.01, 67.96, 67.91, 66.45, 66.41, 66.36, 62.71, 62.68, 62.64, 61.80, 61.73, 39.58, 39.55, 39.52, 39.49, 36.14, 36.11, 34.30, 34.28, 34.15, 32.49, 32.40, 32.04, 32.02, 29.88, 29.82, 29.78, 29.76, 29.64, 29.61, 29.48, 29.44, 29.41, 29.33, 29.25, 29.17, 28.24, 27.34, 27.29, 25.13, 25.11, 24.95, 23.59, 22.81, 19.71, 19.65, 14.25, 13.44. $^{31}$P NMR (202 MHz, $CDCl_3$) δ 69.46, 69.44. HRMS $[C_{52}H_{91}N_4O_8PS + H]^+$: 963.6368 calculated, 963.6387 found.

***O*-(2-(5-(3-(But-3-yn-1-yl)-3*H*-diazirin-3-yl)pentanamido)ethyl)-*O*-((*R*)-2-(oleoyloxy)-3-(palmitoyl-oxy)propyl) phosphorothioate triethylammonium salt (7).**

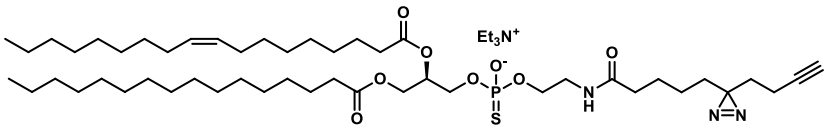

A round bottom flask was charged with thiophosphotriester **49** (29 mg, 30 μmol, 1 eq) and dry DCM (1.5 mL). *tert*-Butylamine (0.5 mL, 4.8 mmol, 160 eq) was added and the reaction mixture was stirred for 3.5 hours, after which the solvent was evaporated. Column chromatography with high-purity grade silica gel (5% MeOH in DCM + 0.5% $Et_3N$) afforded the thiophosphodiester product as the triethylamine salt **7** (8 mg, 7 μmol, 25%). $^1$H NMR (500 MHz, $CDCl_3$ + MeOD) δ 5.36 – 5.26 (m, 2H), 5.25 – 5.19 (m, 1H), 4.37 (dd, *J* = 12.0, 3.3 Hz, 1H), 4.15 (ddd, *J* = 12.0, 6.7, 1.7 Hz, 1H), 4.09 – 3.94 (m, 4H), 3.43 – 3.37 (m, 2H), 3.13 (q, *J* = 7.3 Hz, 6H), 2.29 (q, *J* = 6.9 Hz, 4H), 2.16 – 2.11 (m, 2H), 2.04 (t, *J* = 2.7 Hz, 1H), 2.01 – 1.92 (m, 6H), 1.63 – 1.50 (m, 8H), 1.46 – 1.39 (m, 2H), 1.33 – 1.21 (m, 53H), 1.13 – 1.06 (m, 2H), 0.87 – 0.81 (m, 6H). $^{13}$C NMR (126 MHz, $CDCl_3$ + MeOD) δ 174.60, 174.35, 173.90, 130.35, 130.07, 83.08, 70.78, 70.71, 69.52, 64.92, 64.84, 64.55, 64.50, 64.47, 64.42, 63.05, 46.61, 40.54, 40.49, 36.26, 34.64, 34.50, 32.75, 32.69, 32.30, 32.29, 30.13, 30.07, 30.03, 29.89, 29.73, 29.69, 29.62, 29.52, 29.47, 28.46, 27.56, 27.54, 25.61, 25.28, 25.27, 23.85, 23.03, 14.26, 13.54, 8.85. $^{31}$P NMR (202 MHz, $CDCl_3$ + MeOD) δ 58.38, 58.36. HRMS $[C_{49}H_{87}N_3O_8PS + H]^+$: 910.61025 calculated, 910.61084 found.

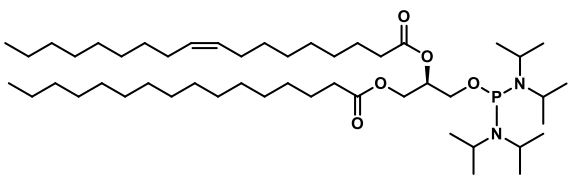

**(*R*)-1-((Bis(diisopropylamino)phosphanyl)oxy)-3-(palmitoyloxy)propan-2-yl oleate (50).** A round bottom flask was charged with **43** (0.28 g, 0.47 mmol, 1 eq), DiPEA (0.27 mL, 1.9 mmol, 4 eq) and dry DCM (2 mL). Bis(diisopropylamino)-chlorophosphine (0.16

g, 0.62 mmol, 1.3 eq) was added. The reaction mixture was stirred for 2 h and then quenched with sat. aq. $NaHCO_3$ in ice (50 mL). EtOAc (100 mL) was added and the organic layer was separated, washed with $H_2O$ (2 x 100 mL) and brine (1 x 100 mL), dried ($Na_2SO_4$), filtered and concentrated under reduced pressure. The crude residue was purified by column chromatography (pre-treat silica with 5% $Et_3N$ in pentane, elute with 2% $Et_3N$ in pentane) affording the phosphordiamidite **50** (0.30 g, 0.36 mmol, 76%). $^1$H NMR (400 MHz, $CDCl_3$) δ 5.40 – 5.28 (m, 2H), 5.18 (p, *J* = 5.0 Hz, 1H), 4.36 (dd, *J* = 11.8, 3.7 Hz, 1H), 4.19 (dd, *J* = 11.7, 6.4 Hz, 1H), 3.66 (t, *J* = 5.7 Hz, 2H), 3.60 – 3.41 (m, 4H), 2.29 (td, *J* = 7.5, 3.4 Hz, 4H), 2.10 – 1.94 (m, 4H), 1.66 – 1.56 (m, 4H), 1.37 – 1.20 (m, 44H), 1.20 – 1.12 (m, 24H), 0.88 (t, *J* = 6.7 Hz, 6H). $^{13}$C NMR (101 MHz, $CDCl_3$) δ 173.50, 173.11, 130.09, 129.82, 71.34, 71.24, 62.93, 62.73, 62.51, 44.67, 44.56, 44.44, 34.49, 34.28, 32.07, 32.05, 29.91, 29.86, 29.84, 29.80, 29.77, 29.67, 29.62, 29.51, 29.46, 29.43, 29.35, 29.28, 29.27, 29.24, 27.35, 27.31, 25.04, 24.76, 24.73, 24.68, 24.65, 23.99, 23.93, 23.87, 22.83, 14.24. $^{31}$P NMR (162 MHz, $CDCl_3$) δ 125.07.

**(*R*)-*O*-(2-(3-(3-(Hex-5-yn-1-yl)-3*H*-diazirin-3-yl)propanamido)ethyl)-*O*-(2-(oleoyloxy)-3-(palmitoyl-oxy)propyl) phosphorodithioate triethylammonium salt (5).**

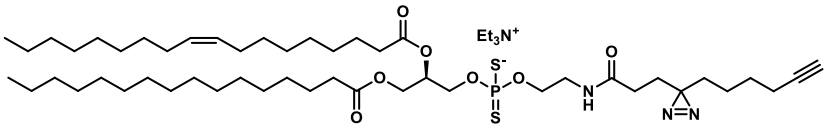


A round bottom flask was charged with diisopropylammonium tetrazolide (12 mg, 71 μmol, 0.55 eq), ethanolamide **38** (31 mg, 0.13 mmol, 1 eq) and dry DCM (1 mL). Phosphordiamidite **50** was taken up in dry DCM (1 mL) and added to the mixture via syringe. The reaction was stirred for 2 h, after which $H_2S$ (0.8 M in THF, 1.6 mL, 1.3 mmol, 10 eq) and 1*H*-tetrazole (0.45 M in $CH_3CN$, 0.57 mL, 0.26 mmol, 2 eq) were added. After stirring for 1 h, argon was bubbled through the reaction mixture and the flow of $H_2S$ was quenched by bleach. $Et_3N$ (0.11 mL, 0.78 mmol, 6 eq) and sulfur ($S_8$, 21 mg, 0.65 mmol, 5 eq) were added and the reaction mixture was stirred overnight. The solvents were evaporated under reduced pressure and the crude residue was purified by column chromatography (97:1:2 -> 94:4:2 DCM/MeOH/AcOH), affording the desired product on $^1$H-NMR and $^{13}$C-NMR but not on $^{31}$P-NMR, suggesting that metals cations were chelating the dithiophosphate. The product was dissolved in a 1:1 mixture of MilliQ and 10% MeOH in $CHCl_3$ (2 mL) and EDTA-$Na_2$ (192 mg, 0.52 mmol, 4 eq) was added. After stirring for 30 min a clear peak was observed again by $^{31}$P-NMR. The mixture was washed with MilliQ (2 x 20 mL) and the combined aqueous layers were back-extracted with 10% MeOH in $CHCl_3$. The combined organic layers were concentrated under reduced pressure and purified by column chromatography with high-purity grade silica gel (1% -> 4% MeOH in DCM + 0.5% $Et_3N$), affording the dithiophosphodiester product as the triethylammonium salt **5** (9.1 μmol, 9.3 mg, 7%). $^1$H NMR (500 MHz, $CDCl_3$ + MeOD) δ 5.36 – 5.27 (m, 2H), 5.27 – 5.21 (m, 1H), 4.38 – 4.35 (m, 1H), 4.17 (dd, *J* = 12.0, 6.6 Hz, 1H), 4.09 (dd, *J* = 9.2, 5.3 Hz, 2H), 4.03 (dt, *J* = 9.8, 5.0 Hz, 2H), 3.46 – 3.39 (m, 2H), 3.21 (q, *J* = 7.3 Hz, 6H), 2.33 – 2.24 (m, 4H), 2.11 (td, *J* = 7.0, 2.6 Hz, 2H), 2.03 – 1.89 (m, 7H), 1.73 – 1.65 (m, 2H), 1.62 – 1.53 (m, 4H), 1.47 – 1.41 (m, 2H), 1.41 – 1.37 (m, 2H), 1.35 (t, *J* = 7.3 Hz, 9H), 1.31 – 1.18 (m, 46H), 0.84 (t, *J* = 6.8 Hz, 6H). $^{13}$C NMR (126 MHz, $CDCl_3$ + MeOD) δ 174.35, 173.92, 173.07, 130.27, 130.02, 84.16, 70.67, 70.59, 68.95, 64.84, 64.78, 63.98, 63.93, 63.13, 62.60, 46.92, 40.29, 40.24, 34.60, 34.46, 32.43, 32.24, 32.22, 30.60, 30.06, 30.05, 30.01, 29.98, 29.97, 29.83, 29.68, 29.63, 29.61, 29.56, 29.47, 29.45, 29.41, 29.26, 28.59, 28.17, 27.50, 27.48, 25.21, 23.23, 22.98, 18.39, 14.25, 8.93. $^{31}$P NMR (202 MHz, $CDCl_3$ + MeOD) δ 114.99. HRMS $[C_{49}H_{88}N_3O_7PS_2 + H]^+$: 926.5874 calculated, 926.5878 found.

*LEI-401-based photoprobes **51-52***

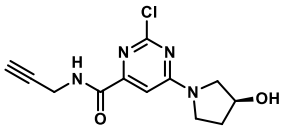

**(*S*)-2-Chloro-6-(3-hydroxypyrrolidin-1-yl)-*N*-(prop-2-yn-1-yl)pyrimidine-4-carboxamide (54).** A round bottom flask was charged with dichloropyrimidine **53** (described in Chapter 3, 138 mg, 0.60 mmol, 1 eq) and MeOH (3 mL) and cooled to 0 °C. DiPEA (261 μL, 1.5 mmol, 2.5 eq) and (*S*)-3-hydroxypyrrolidine HCl salt (78 mg, 0.63 mmol, 1.05 eq) were added and the reaction was stirred for 1.5 hours after which the solvents were evaporated. The residue was purified by silica gel column chromatography (80% -> 100% EtOAc/pentane) affording the product **54** (139 mg, 0.50 mmol, 83%). TLC: $R_f$ = 0.2 (90% EtOAc/pentane). $^1$H NMR (400 MHz, $CDCl_3$) δ 8.13 (t, *J* = 5.6 Hz, 1H), 7.06 – 6.89 (m, 1H), 4.73 – 4.57 (m, 1H), 4.29 – 4.15 (m, 2H), 3.88 – 3.19 (m, 5H), 2.33 (t, *J* = 2.5 Hz, 1H), 2.23 – 2.07 (m, 2H). $^{13}$C NMR (101 MHz, $CDCl_3$) δ 162.58, 162.16, 162.01, 159.71, 159.59, 155.59, 100.70, 100.64, 78.74, 72.13, 70.43, 69.73, 55.57, 55.28, 45.29, 45.03, 33.79, 33.26, 29.28. HRMS $[C_{12}H_{13}ClN_4O_2 + H]^+$: 281.0800 calculated, 281.0796 found.

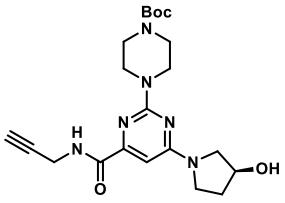

***tert*-Butyl (*S*)-4-(4-(3-hydroxypyrrolidin-1-yl)-6-(prop-2-yn-1-ylcarbamoyl)-pyrimidin-2-yl)piperazine-1 carboxylate (55).** A round bottom flask was charged with 2-chloropyrimidine **54** (117 mg, 0.42 mmol, 1 eq), DiPEA (218 μL, 1.25 mmol, 3 eq), 1-Boc-piperazine (110 mg, 0.59 mmol, 1.4 eq) and *n*-BuOH (2 mL). The reaction was stirred at 100 °C for 48 h, after which the solvents were evaporated. The residue was purified by silica gel column chromatography (80% -> 100% EtOAc/pentane) affording the product **55** (163 mg, 0.38 mmol, 90%). TLC: $R_f$ = 0.3 (90% EtOAc/pentane). $^1$H NMR (400 MHz, $CDCl_3$) δ 8.10 (t, *J* = 5.4 Hz, 1H), 6.63 – 6.27 (m, 1H), 4.56 (s, 1H), 4.20 (dd, *J* = 5.5, 2.2 Hz, 2H), 3.88 – 3.69 (m, 5H), 3.69 – 3.51 (m, 3H), 3.51 – 3.35 (m, 5H), 2.31 (t, *J* = 2.4 Hz, 1H), 2.19 – 1.95 (m, 2H), 1.49 (s, 9H). $^{13}$C NMR (101 MHz, $CDCl_3$) δ 164.62, 161.73, 160.68, 154.88, 154.51, 92.43, 79.97, 79.37, 71.64, 70.56, 69.81, 54.74, 44.36, 43.67, 34.00, 33.16, 28.99, 28.42. HRMS $[C_{21}H_{30}N_6O_4 + H]^+$: 431.2401 calculated, 431.2397 found.

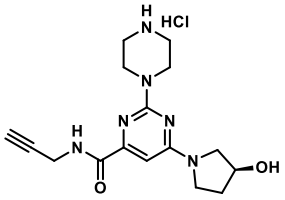

(***S*)-6-(3-Hydroxypyrrolidin-1-yl)-2-(piperazin-1-yl)-*N*-(prop-2-yn-1-yl)pyrimidine-4-carboxamide (56).** A round bottom flask was charged with Boc-piperazine **55** (160 mg, 0.37 mmol, 1 eq) and 4 M HCl in dioxane (2 mL, 8 mmol, 21 eq). After stirring for 2 h at rt the solvents were evaporated under reduced pressure affording the HCl salt **56**, which was used for the next step without further purification (135 mg, 0.37 mmol, quant.)

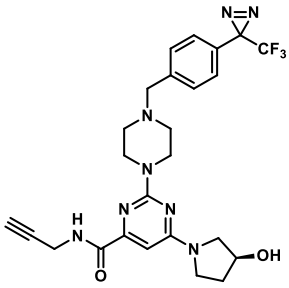

**(*S*)-6-(3-Hydroxypyrrolidin-1-yl)-*N*-(prop-2-yn-1-yl)-2-(4-(4-(3-(trifluoromethyl)-3*H*-diazirin-3-yl)benzyl)piperazin-1-yl)pyrimidine-4-carboxamide (51).** A round bottom flask was charged with amine HCl salt **56** (26 mg, 45 μmol, 1 eq) in dry $CH_3CN$ (1 mL). This was followed by addition of DiPEA (37 μL, 0.21 mmol, 3 eq) and 4-[3-(trifluoromethyl)-3H-diazirin-3-yl]benzyl bromide (14 μL, 85 μmol, 1.2 eq). The reaction was stirred in the dark for 3 h at rt after which the solvents were evaporated under reduced pressure. The residue was purified by silica gel column chromatography (2.5 -> 7.5% MeOH/DCM) affording the product **51** (12 mg, 23 μmol, 32%). TLC: $R_f$ = 0.4 (5% MeOH/DCM). $^1$H NMR (500 MHz, $CDCl_3$) δ 7.99 (t, *J* = 5.5 Hz, 1H), 7.40 (d, *J* = 8.2 Hz, 2H), 7.16 (d, *J* = 8.0 Hz, 2H), 6.54 (s, 1H), 4.58 (br s, 1H), 4.20 (dd, *J* = 5.6, 2.5 Hz, 2H), 3.80 (br s, 4H), 3.62 (br s, 2H), 3.56 (s, 2H), 3.43 (s, 1H), 2.58 – 2.34 (m, 4H), 2.25 (t, *J* = 2.5 Hz, 1H), 2.08 (br s, 2H), 1.71 (br s, 2H). $^{13}$C NMR (126 MHz, $CDCl_3$) δ 122.28 (q, *J* = 274.7, 273.4 Hz). $^{13}$C NMR (126 MHz, $CDCl_3$) δ 164.73, 162.05, 160.92, 154.93, 140.07, 129.66, 128.09, 126.55, 122.28 (q, *J* = 274.4 Hz), 92.22, 79.56, 71.65, 70.36, 62.62, 54.92, 53.17, 44.36, 43.91, 34.25, 29.15, 28.51 (q, *J* = 40.4 Hz). HRMS $[C_{25}H_{27}F_3N_8O_2 + H]^+$: 529.2282 calculated, 529.2296 found.

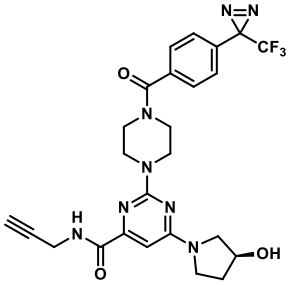

**(*S*)-6-(3-Hydroxypyrrolidin-1-yl)-*N*-(prop-2-yn-1-yl)-2-(4-(4-(3-(trifluoromethyl)-3*H*-diazirin-3-yl)benzoyl)piperazin-1-yl)pyrimidine-4-carboxamide (52).** A round bottom flask was charged with amine HCl salt **56** (30 mg, 82 μmol, 1 eq) in dry DMF (1 mL) at 0 °C. This was followed by addition of DiPEA (57 μL, 0.33 mmol, 4 eq), 4-[3-(trifluoromethyl)-3H-diazirin-3-yl]benzoic acid (19 mg, 82 μmol, 1.2 eq) and PyBOP (47 mg, 90 μmol, 1.1 eq). The reaction was stirred in the dark overnight warming up to rt after which the solvents were evaporated under reduced pressure and the residue was coevaporated with toluene. The residue was purified by silica gel column chromatography (2.5 -> 7.5% MeOH/DCM) affording the product **52** (8 mg, 15 μmol, 18%). TLC: $R_f$ = 0.5 (100% EtOAc). $^1$H NMR (500 MHz, MeOD) δ 7.58 (d, *J* = 8.5 Hz, 2H), 7.38 (d, *J* = 8.1 Hz, 2H), 6.60 – 6.40 (m, 1H), 4.59 – 4.41 (m, 1H), 4.18 – 4.07 (m, 2H), 3.97 (br s, 2H), 3.83 (br s, 4H), 3.76 – 3.49 (m, 4H), 3.49 – 3.34 (m, 2H), 2.58 (t, *J* = 2.5 Hz, 1H), 2.22 – 1.91 (m, 2H). $^{13}$C NMR (126 MHz, MeOD) δ 171.27, 166.81, 163.30, 162.25, 156.47, 138.57, 131.69, 128.99, 127.98, 123.47 (q, *J* = 273.7 Hz), 93.19, 80.63, 79.48, 71.91, 70.77, 55.53, 45.34, 44.64, 43.49, 34.73, 34.02, 29.44 (d, *J* = 40.5 Hz), 29.43. HRMS $[C_{25}H_{25}F_3N_8O_3 + H]^+$: 543.2075 calculated, 543.2085 found.

## References


1. Durham, T.B. & Wiley, M.R. Target engagement measures in preclinical drug discovery: theory, methods, and case studies, in *Translating Molecules into Medicines: Cross-Functional Integration at the Drug Discovery-Development Interface*. (eds. S.N. Bhattachar, J.S. Morrison, D.R. Mudra & D.M. Bender) 41-80 (Springer International Publishing, Cham; 2017).
2. Simon, G.M., Niphakis, M.J. & Cravatt, B.F. Determining target engagement in living systems. *Nature Chemical Biology* **9**, 200 (2013).
3. Cummings, J. Lessons learned from Alzheimer disease: clinical trials with negative outcomes. *Clinical and Translational Science* **11**, 147-152 (2018).
4. McClure, R.A. & Williams, J.D. Impact of mass spectrometry-based technologies and strategies on chemoproteomics as a tool for drug discovery. *ACS Medicinal Chemistry Letters* **9**, 785-791 (2018).
5. Niphakis, M.J. & Cravatt, B.F. Enzyme inhibitor discovery by activity-based protein profiling. *Annual Review of Biochemistry* **83**, 341-377 (2014).
6. Willems, L.I., Overkleeft, H.S. & van Kasteren, S.I. Current developments in activity-based protein profiling. *Bioconjugate Chemistry* **25**, 1181-1191 (2014).
7. Baggelaar, M.P., Chameau, P.J.P., Kantae, V., Hummel, J., Hsu, K.L., Janssen, F., van der Wel, T., Soethoudt, M., Deng, H., den Dulk, H., Allara, M., Florea, B.I., Di Marzo, V., Wadman, W.J., Kruse, C.G., Overkleeft, H.S., Hankemeier, T., Werkman, T.R., Cravatt, B.F. & van der Stelt, M. Highly selective, reversible inhibitor identified by comparative chemoproteomics modulates diacylglycerol lipase activity in neurons. *J. Am. Chem. Soc.* **137**, 8851-8857 (2015).
8. Baggelaar, M.P., Janssen, F.J., van Esbroeck, A.C.M., den Dulk, H., Allara, M., Hoogendoorn, S., McGuire, R., Florea, B.I., Meeuwenoord, N., van den Elst, H., van der Marel, G.A., Brouwer, J., Di Marzo, V., Overkleeft, H.S. & van der Stelt, M. Development of an activity-based probe and *in silico* design reveal highly selective inhibitors for diacylglycerol lipase-alpha in brain. *Angew. Chem.-Int. Edit.* **52**, 12081-12085 (2013).
9. Ogasawara, D., Deng, H., Viader, A., Baggelaar, M.P., Breman, A., den Dulk, H., van den Nieuwendijk, A.M.C.H., Soethoudt, M., van der Wel, T., Zhou, J., Overkleeft, H.S., Sanchez-Alavez, M., Mori, S., Nguyen, W., Conti, B., Liu, X., Chen, Y., Liu, Q.-s., Cravatt, B.F. & van der Stelt, M. Rapid and profound

rewiring of brain lipid signaling networks by acute diacylglycerol lipase inhibition. *Proceedings of the National Academy of Sciences* **113**, 26 (2016).

10. van Esbroeck, A.C.M., Janssen, A.P.A., Cognetta, A.B., Ogasawara, D., Shpak, G., van der Kroeg, M., Kantae, V., Baggelaar, M.P., de Vrij, F.M.S., Deng, H., Allara, M., Fezza, F., Lin, Z., van der Wel, T., Soethoudt, M., Mock, E.D., den Dulk, H., Baak, I.L., Florea, B.I., Hendriks, G., de Petrocellis, L., Overkleeft, H.S., Hankemeier, T., De Zeeuw, C.I., Di Marzo, V., Maccarrone, M., Cravatt, B.F., Kushner, S.A. & van der Stelt, M. Activity-based protein profiling reveals off-target proteins of the FAAH inhibitor BIA 10-2474. *Science* **356**, 1084-1087 (2017).
11. van Rooden, E.J., Florea, B.I., Deng, H., Baggelaar, M.P., van Esbroeck, A.C.M., Zhou, J., Overkleeft, H.S. & van der Stelt, M. Mapping *in vivo* target interaction profiles of covalent inhibitors using chemical proteomics with label-free quantification. *Nature Protocols* **13**, 752 (2018).
12. Geurink, P.P., Prely, L.M., van der Marel, G.A., Bischoff, R. & Overkleeft, H.S. Photoaffinity labeling in activity-based protein profiling. *Top. Curr. Chem.* **324**, 85-113 (2012).
13. Lapinsky, D.J. & Johnson, D.S. Recent developments and applications of clickable photoprobes in medicinal chemistry and chemical biology. *Future Medicinal Chemistry* **7**, 2143-2171 (2015).
14. Pan, S., Zhang, H., Wang, C., Yao, S.C.L. & Yao, S.Q. Target identification of natural products and bioactive compounds using affinity-based probes. *Natural Product Reports* **33**, 612-620 (2016).
15. Wright, M.H. & Sieber, S.A. Chemical proteomics approaches for identifying the cellular targets of natural products. *Natural Product Reports* **33**, 681-708 (2016).
16. Flaxman, H.A. & Woo, C.M. Mapping the small molecule interactome by mass spectrometry. *Biochemistry* **57**, 186-193 (2018).
17. Smith, E. & Collins, I. Photoaffinity labeling in target- and binding-site identification. *Future Medicinal Chemistry* **7**, 159-183 (2015).
18. Xia, Y. & Peng, L. Photoactivatable lipid probes for studying biomembranes by photoaffinity labeling. *Chemical Reviews* **113**, 7880-7929 (2013).
19. Haberkant, P. & Holthuis, J.C.M. Fat & fabulous: Bifunctional lipids in the spotlight. *Biochimica et Biophysica Acta (BBA) - Molecular and Cell Biology of Lipids* (2014).
20. Murale, D.P., Hong, S.C., Haque, M.M. & Lee, J.-S. Photo-affinity labeling (PAL) in chemical proteomics: a handy tool to investigate protein-protein interactions (PPIs). *Proteome Science* **15**, 14 (2017).
21. Das, J. Aliphatic diazirines as photoaffinity probes for proteins: recent developments. *Chemical Reviews* **111**, 4405-4417 (2011).
22. Dubinsky, L., Krom, B.P. & Meijler, M.M. Diazirine based photoaffinity labeling. *Bioorganic & Medicinal Chemistry* **20**, 554-570 (2012).
23. Ge, S.-S., Chen, B., Wu, Y.-Y., Long, Q.-S., Zhao, Y.-L., Wang, P.-Y. & Yang, S. Current advances of carbene-mediated photoaffinity labeling in medicinal chemistry. *RSC Advances* **8**, 29428-29454 (2018).
24. Nickon, A. New perspectives on carbene rearrangements: migratory aptitudes, bystander assistance, and geminal efficiency. *Accounts of Chemical Research* **26**, 84-89 (1993).
25. Tanaka, Y., Bond, M.R. & Kohler, J.J. Photocrosslinkers illuminate interactions in living cells. *Molecular BioSystems* **4**, 473-480 (2008).
26. Saghatelian, A., Jessani, N., Joseph, A., Humphrey, M. & Cravatt, B.F. Activity-based probes for the proteomic profiling of metalloproteases. *Proceedings of the National Academy of Sciences of the United States of America* **101**, 10000-10005 (2004).
27. Shi, H., Cheng, X., Sze, S.K. & Yao, S.Q. Proteome profiling reveals potential cellular targets of staurosporine using a clickable cell-permeable probe. *Chemical Communications* **47**, 11306-11308 (2011).
28. Crump, C.J., Murrey, H.E., Ballard, T.E., am Ende, C.W., Wu, X., Gertsik, N., Johnson, D.S. & Li, Y.-M. Development of sulfonamide photoaffinity inhibitors for probing cellular γ-secretase. *ACS Chemical Neuroscience* **7**, 1166-1173 (2016).

29. Horning, B.D., Suciu, R.M., Ghadiri, D.A., Ulanovskaya, O.A., Matthews, M.L., Lum, K.M., Backus, K.M., Brown, S.J., Rosen, H. & Cravatt, B.F. Chemical proteomic profiling of human methyltransferases. *J. Am. Chem. Soc.* **138**, 13335-13343 (2016).
30. Soethoudt, M., Stolze, S.C., Westphal, M.V., van Stralen, L., Martella, A., van Rooden, E.J., Guba, W., Varga, Z.V., Deng, H., van Kasteren, S.I., Grether, U., Ijzerman, A.P., Pacher, P., Carreira, E.M., Overkleeft, H.S., Ioan-Facsinay, A., Heitman, L.H. & van der Stelt, M. Selective photoaffinity probe that enables assessment of cannabinoid $CB_2$ receptor expression and ligand engagement in human cells. *J. Am. Chem. Soc.* **140**, 6067-6075 (2018).
31. Xie, Y., Ge, J., Lei, H., Peng, B., Zhang, H., Wang, D., Pan, S., Chen, G., Chen, L., Wang, Y., Hao, Q., Yao, S.Q. & Sun, H. Fluorescent probes for single-step detection and proteomic profiling of histone deacetylases. *J. Am. Chem. Soc.* **138**, 15596-15604 (2016).
32. Keow, J.Y., Pond, E.D., Cisar, J.S., Cravatt, B.F. & Crawford, B.D. Activity-based labeling of matrix metalloproteinases in living vertebrate embryos. *PLoS ONE* **7**, e43434 (2012).
33. Chicca, A., Nicolussi, S., Bartholomäus, R., Blunder, M., Aparisi Rey, A., Petrucci, V., Reynoso-Moreno, I.d.C., Viveros-Paredes, J.M., Dalghi Gens, M., Lutz, B., Schiöth, H.B., Soeberdt, M., Abels, C., Charles, R.-P., Altmann, K.-H. & Gertsch, J. Chemical probes to potently and selectively inhibit endocannabinoid cellular reuptake. *Proceedings of the National Academy of Sciences* **114**, E5006-E5015 (2017).
34. Okamoto, Y., Morishita, J., Tsuboi, K., Tonai, T. & Ueda, N. Molecular characterization of a phospholipase D generating anandamide and its congeners. *Journal of Biological Chemistry* **279**, 5298-5305 (2004).
35. Magotti, P., Bauer, I., Igarashi, M., Babagoli, M., Marotta, R., Piomelli, D. & Garau, G. Structure of human *N*-acylphosphatidylethanolamine-hydrolyzing phospholipase D: regulation of fatty acid ethanolamide biosynthesis by bile acids. *Structure* **23**, 598-604 (2015).
36. Petersen, G., Pedersen, A.H., Pickering, D.S., Begtrup, M. & Hansen, H.S. Effect of synthetic and natural phospholipids on *N*-acylphosphatidylethanolamine-hydrolyzing phospholipase D activity. *Chemistry and Physics of Lipids* **162**, 53-61 (2009).
37. Wang, J., Okamoto, Y., Morishita, J., Tsuboi, K., Miyatake, A. & Ueda, N. Functional analysis of the purified anandamide-generating phospholipase D as a member of the metallo-β-lactamase family. *Journal of Biological Chemistry* **281**, 12325-12335 (2006).
38. Astarita, G., Ahmed, F. & Piomelli, D. Identification of biosynthetic precursors for the endocannabinoid anandamide in the rat brain. *Journal of Lipid Research* **49**, 48-57 (2008).
39. Müller, S., Liepold, B., Roth, G.J. & Bestmann, H.J. An improved one-pot procedure for the synthesis of alkynes from aldehydes. *Synlett* **1996**, 521-522 (1996).
40. Fodran, P. & Minnaard, A.J. Catalytic synthesis of enantiopure mixed diacylglycerols - synthesis of a major M. tuberculosis phospholipid and platelet activating factor. *Organic & Biomolecular Chemistry* **11**, 6919-6928 (2013).
41. Bond, M.R., Zhang, H., Vu, P.D. & Kohler, J.J. Photocrosslinking of glycoconjugates using metabolically incorporated diazirine-containing sugars. *Nature Protocols* **4**, 1044 (2009).
42. Pongracz, K. & Gryaznov, S. Oligonucleotide N3'→P5' thiophosphoramidates: synthesis and properties. *Tetrahedron Letters* **40**, 7661-7664 (1999).
43. Franklin, C.L., Li, H. & Martin, S.F. Design, synthesis, and evaluation of water-soluble phospholipid analogues as inhibitors of phospholipase C from Bacillus cereus. *The Journal of Organic Chemistry* **68**, 7298-7307 (2003).
44. Prestwich, G.D., Xu, Y., Qian, L., Gajewiak, J. & Jiang, G. New metabolically stabilized analogues of lysophosphatidic acid: agonists, antagonists and enzyme inhibitors. *Biochemical Society Transactions* **33**, 1357-1361 (2005).
45. Yang, X. & Mierzejewski, E. Synthesis of nucleoside and oligonucleoside dithiophosphates. *New Journal of Chemistry* **34**, 805-819 (2010).

46. Guga, P. & Koziołkiewicz, M. Phosphorothioate nucleotides and oligonucleotides – recent progress in synthesis and application. *Chemistry & Biodiversity* **8**, 1642-1681 (2011).
47. Barone, A.D., Tang, J.Y. & Caruthers, M.H. In situ activation of bis-dialkylaminophosphines--a new method for synthesizing deoxyoligonucleotides on polymer supports. *Nucleic acids research* **12**, 4051-4061 (1984).
48. Rappsilber, J., Mann, M. & Ishihama, Y. Protocol for micro-purification, enrichment, pre-fractionation and storage of peptides for proteomics using StageTips. *Nature Protocols* **2**, 1896 (2007).
49. Distler, U., Kuharev, J., Navarro, P. & Tenzer, S. Label-free quantification in ion mobility–enhanced data-independent acquisition proteomics. *Nature Protocols* **11**, 795 (2016).
50. Rawling, T., Duke, C.C., Cui, P.H. & Murray, M. Facile and stereoselective synthesis of (Z)-15-octadecenoic acid and (Z)-16-nonadecenoic acid: monounsaturated omega-3 fatty acids. *Lipids* **45**, 159-165 (2010).
51. Ahad, A.M., Jensen, S.M. & Jewett, J.C. A traceless Staudinger reagent to deliver diazirines. *Organic Letters* **15**, 5060-5063 (2013).